Review article

Synthesis of silica and silicon from rice husk feedstock: A review

Ibrahim Hamidu [a,b,*], Benjamin Afotey [a], Bright Kwakye-Awuah [c],
Daniel Adjah Anang [a]

[a] *Department of Chemical Engineering, Kwame Nkrumah University of Science and Technology, Kumasi, Ghana*
[b] *Department of Chemical Sciences, University of Development Studies, Nyankpala Campus, Ghana*
[c] *Department of Physics, Kwame Nkrumah University of Science and Technology, Kumasi, Ghana*

ARTICLE INFO

ABSTRACT

A lot of attention has been drawn to environmentally friendly and sustainable materials in the need to decarbonize the planet. The utilization of agro-waste to meet this need has increased in recent times. Among the various agro-wastes, rice husk has gained more traction due to its abundance, unique constituents, and properties suitable for advanced material synthesis. Precursor materials such as silica and silicon used in advanced materials synthesis are also synthesized from rice husk. The synthesis of these advanced materials depends on the rice husk pretreatment and thermochemical conversion approach. Pretreatment methods such as acid leaching generally yield higher silica purity compared to water leaching. However, the use of acid in leaching impurities during pretreatment leads to the release of harmful chemicals. Among thermochemical methods used in silica synthesis, the hydrothermal method has gained more attention due to the use of water as a liquid medium and the elimination of the raw materials drying step, reducing emissions and energy demand in the process. Metallothermic reduction methods such as magnesiothermic and aluminothermic reduction of silica to silicon have attracted much attention due to their low reduction temperature. This review discusses the composition and properties of rice husk and its thermochemical conversion to silica (SiO_2) and silicon (Si). Silica and silicon are essential materials used as framework or precursor materials in the synthesis of other advanced materials such as zeolites and catalyst supports. The second part of the review discusses the various thermochemical conversion approaches and their kinetics. The final part of the review discusses the various rice husk-derived advanced materials and their applications.

1. Introduction

Despite silica being the most abundant oxide in the Earth's crust, it is synthesized for its technological applications [1]. The conventional method of synthesizing spherical silica from quartz using vapor-phase synthesis and spheroidizing processes yields highly fluid and dense spherical silica powder. However, this powder is radioactive due to the quartz used as the raw material [2].

In conventional silica production from quartz, for every 1 ton of silica produced, 0.51 tons of sulfuric acid and 0.53 tons of sodium carbonate are used, resulting in the release of 0.23 tons of carbon dioxide, 0.74 tons of sodium sulfate, and 20 tons of wastewater. The conventional silica production process from quartz is highly energy-intensive and environmentally unfriendly due to the release of

---

large amounts of CO_2 and salts [3].

Tetraethyloxysilane (TEOS) and tetramethyloxysilane (TMOS) are among the conventional precursor materials used in nanosilica synthesis, but they are expensive, toxic, and environmentally unfriendly [4–6]. Therefore, it is necessary to explore and develop less energy-intensive processes that translate to lower costs and carbon emissions.

Rice husk, an agro-waste, provides a cheap, less energy-consuming, and environmentally friendly precursor material for the synthesis of amorphous silica [7,8]. The use of rice husk as a valuable precursor material not only solves the disposal problem but also enables the recovery of essential materials [9]. Although the use of rice husk as a silica synthesis precursor material has enormous environmental benefits, such as carbon reduction, it is not economically beneficial. However, an intermediate energy generation step from the conversion of rice husk can make it economically viable [10].

The thermochemical processes used in the conversion of rice husk to valuable precursor materials, such as rice husk ash, also pose numerous challenges. Among these challenges are the bulk nature of rice husk and its hard surface. Additionally, the high amount of silicon in rice husk and the inability of bacteria to degrade it make its residue a source of pollution in the environment [11]. The effective utilization of this residue in valuable materials, such as silica and silicon synthesis, provides an additional advantage.

The projected global population growth and urbanization will translate to an increase in energy demand, which will also lead to an increase in greenhouse gas emissions [12]. The global agricultural production demand due to population increase (to over 9 billion) by 2050 is also projected to increase by 60 % based on 2005–2007 production levels [13]. Hence, the continued increase in food production, especially rice, which is a staple food, makes rice husk a renewable and abundant resource. Although there is a release of carbon dioxide in the thermochemical conversion of rice husk, the carbon impact of the entire process is, however, carbon neutral or negative [11].

As temperature increases during the thermochemical conversion process, silica accumulates as carbon reduces [14]. The silica content in rice husk ash can increase from 85-95 % to 90–98 % silica upon complete combustion [9]. In complete combustion, all the organic components within the rice husk are removed, leaving inorganics highly rich in silica.

Among the methods for extracting silica from rice husk are sol-gel and precipitation [5]. Rice husk ash, which is rich in silica, also contains various alkali impurities that reduce the silica purity. Biobased silica synthesized from rice husk ash contains varying levels of CaO, K_2O, MgO, and Al_2O_3 impurities, which can be removed via water, acid, and alkali leaching [15]. During the ashing of raw rice husk, carbon that gets trapped in the silica melt in the presence of K_2O impurities does not oxidize, as it does not have direct interaction with air. This carbon fixation increases with an increase in calcination temperature, leading to a large amount of black particles (unburnt carbon) wrapped in the silica [16]. Fig. 2 shows the schematic of the integrated silica and silicon synthesis from rice husk feedstock. As indicated in Fig. 2, the extraction of silica and subsequent reduction of silica to silicon occurs after the impurities removal stage a through pretreatment process.

Understanding the biosilification process in rice, which leads to the accumulation of silicon within the rice husk, is crucial in the silica extraction process. The biosilification process also highlights the various molecules and possible functional groups present in silica synthesized from rice husk sources. Additionally, the biosilification process leads to the formation of a lignocellulose network within the rice plant [13].

1.1. Silica formation and absorption

Silicon is the second most abundant element in the Earth's crust, after oxygen, and is released into the soil through chemical and biological processes [14]. There is also a continuous process of hydration and dehydration of silica within the Earth's biosphere, involving a reversible pH-dependent hydrolysis and condensation process. Soluble silicic acid is produced as a result, which dehydrates to form amorphous silica nanoparticles with 2–8 membered siloxane rings [17]. The reaction process is as follows [17]:

$$(SiO_2)_x + 2H_2O \leftrightarrow (SiO_2)_{x-1} + Si(OH)_4$$
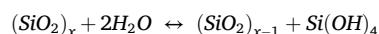
Rice, which belongs to the Graminae family, absorbs monosilicic acid $(Si(OH)_4)$ within its cells as a hydrated deposit [9,18]. Silicon enters rice plants through their roots in soluble monosilicic acid and/or silicate forms, which undergo biomineralization/biosilification to form silica and lignocellulose networking [13].

Silicon, an essential mineral for plant growth, is bonded with hemicellulose (a complex mixture of branched-chain and heterogeneous polysaccharides) [19]. The silica content is inversely correlated with cellulose and lignin in wetland macrophytes [2]. Phytoliths, which are the silicon accumulations in plants, primarily consist of amorphous silica in hydrated form with 5–15 % water [14].

The silica is deposited within the cell walls, forming silica-cellulose double layers and silica cuticles on the surfaces of leaves, husks, and stems [14,20]. The silicon/silica within rice plants enhances their mechanical strength, rigidity, stiffness, and resistance to biotic and abiotic stresses, such as pests, diseases, predators, and fungal defense [2,13]. Silica, which occurs in hydrated form within rice, constitutes 8.7 %–12.1 %, averaging 10.6 %, and is mainly found in the husk of the rice [14]. Silicon, when accumulated in excess, does not damage the plant [13].

1.2. Rice husk composition and properties

Rice husk, an agro-waste from rice production, presents advantages in decarbonization [21]. Rice absorbs carbon dioxide during its growth, which is released during the thermochemical conversion of rice husk, making it almost carbon neutral [11]. Rice husk ash is a

bulky, lightweight, and porous material with a density of 180–200 kg/m³ and a specific gravity (of ground rice husk ash) between 2 and 2.5, depending on the fineness level [16]. The density of black and white rice husk ash is 1.8 and 2.2 g/cm³, respectively, with an average RHA density of 2.11 g/cm³ [13]. Agricultural waste, such as rice husk, contains 80 % organics, with the remaining portion consisting of toxic waste (e.g., herbicides, insecticides, and pesticides) [22]. Lignocellulose biomass (e.g., rice husk) primarily contains cellulose, lignin, and hemicellulose components [23]. Rice husk accounts for 20–33 % of paddy weight, with a 72–85 wt% ligno-cellulose content [13]. Table 1 shows literature data on the organic and inorganic compositions of rice husk.

Rice husk (RH) contains 15.3–24.6 % ash content (dry weight basis) after combustion, has a refractive index of 1.44, and a heating value of 13–16 MJ/kg [24–26]. Various higher heating values, proximate analysis, and ultimate analysis from the literature are shown in Table 3. Rice husk, which contains approximately 15–25 % silica, is affected by climate, rice variety, and geographic location of cultivation [27].

Cellulose, a major constituent of rice husk, yields carbon during thermal decomposition in an inert atmosphere [33]. Hemicellulose is less stable than lignin and cellulose and degrades at much lower temperatures compared to lignin and cellulose [34]. The monomeric components of hemicellulose are responsible for the production of materials such as activated carbon, silica, and xylose due to polarity from an electromeric effect [3]. Cellulose decomposes between 275 and 350 °C, whereas hemicellulose decomposes between 150 and 350 °C (due to its lower stability compared to cellulose) [31]. The organic components of rice husk are thermally destructed completely in the temperature range of 470–730 °C [8]. The various thermo-gravimetric stages and corresponding temperature ranges of rice husk corresponding to the various components are shown in Table 2.

Typically, rice husk contains approximately 20 % silica, while rice husk ash (RHA) contains approximately 90 % amorphous silica [21]. Silica is the main component of rice husk ash, with trace amounts of CaO, Na_2O, MgO, K_2O, Fe_2O_3, and Al_2O_3 [13,31]. Various rice husk chemical composition data from the literature are shown in Table 4. The RHA contains 90–97 % opal-type amorphous silica [24]. The literature composition data of silica in rice husk and rice husk ash are shown in Table 2.

1.3. General rice husk/rice husk ash application

Silica is used in the synthesis of silicon-based materials, such as silicon tetrachloride [28], as biosensors, catalysts, fillers, pesticides [27], zeolites synthesis, fillers in polymer composites, ceramics production, adsorbent materials [8], and tire production [21]. As shown in Fig. 1, amorphous rice husk silica is useful in various industries, such as the rubber, activated carbons, energy storage materials, drug delivery, carbon capture materials, glass making, steel, cement, pharmaceuticals, paints, soap [13,35], pozzolan in cement [36], and silicon integrated circuit insulators [37]. Various indicators influence rice husk use, such as chemical purity for advanced material synthesis and reactivity for pozzolan in cements and concrete [38].

Nanosilica is used in detergents, adhesives, pesticides, ceramics, medicines, and vegetable oil refineries [5], chromatography [7], and corrosion inhibition [34]. Spherical silica is highly useful in the packaging industry due to its electrical and thermal insulation and low thermal expansion coefficient. The hierarchical structure of spherical silica micro/macro powder makes it ideal for medical, biological, and catalytic applications [2].

Surface-modified silica nanoparticles (20 nm particle size) with a narrow particle size distribution are used as epoxy resin concentrates (fillers), adhesives, and as composites in machine and automotive parts to improve their toughness, modulus, fatigue performance, and strength. A 10 wt% addition of silica nanoparticles improves fatigue performance, increases compressive strength by 10–30 %, modulus by 30–50 %, and fracture toughness (K_{ic}) by 50 % [39].

1.4. Rice husk impurities and impurities treatment

Rice husk ash contains 82–98 % silica [40], with trace amounts of Al_2O_3, Fe_2O_3, K_2O, CaO, and Na_2O impurities [28,31,40]. Acids (HCl, HNO_3, H_2SO_4, H_3PO_4, CH_3COOH) and alkali (NaOH, KOH, $Ca(OH)_2$) leaching remove metallic impurities, yielding higher purity amorphous silica [34]. Metallic impurities such as sodium (Na), potassium (K), calcium (Ca), magnesium (Mg), iron (Fe), and manganese (Mn) found in rice husk can be removed through acid pretreatment [31] and yield ash silica that is completely white in color with a high surface area [3]. The effect of impurities leaching on the composition of silica compared to as-received rice husk is shown in

Table 1
Organic and inorganic composition of rice husk.

Organic components (wt. %)				Inorganics/Silica (wt. %)	reference
Polysaccharide		Lignin	Other extractives		
Cellulose	Hemicellulose				
50	n/a	25–30	n/a	15–20	[18]
35–40	15–20	20–25	n/a	15–28	[13]
40–50	n/a	25–30	n/a	15–20	[28]
37.34	10.07	41.08	11.31	n/a	[29]
55–60		22	n/a	n/a	[30]
70–80			n/a	20–30	[10]
70–90			n/a	17–20	[31]
75–90			n/a	10–20	[32]

Table 2

Decomposition temperature ranges for the components of rice husk.

Stage	Activity	Temperature (°C)	Weight loss (%)	Reference
I	Water removal	80–120	1–2	[24]
	Endothermic water removal	90	n/a	[8]
	No noticeable weight loss	120–220	n/a	[24]
	Rice husk dehydration, due to water loss	100	n/a	[34]
	Negligible weight loss	120–210	n/a	[34]
	Water removal	50–150	1–2	[31]
II	Cellulose and hemicellulose organic component, and other volatile organic component removal	220–370	26–31	[24]
	Exothermic thermal destruction of cellulose, hemicellulose	330	n/a	[8]
	Thermal decomposition of cellulose and hemicellulose, resulting in volatile organic compounds	210–350	n/a	[34]
	Thermal decomposition of cellulose and hemicellulose	240–360	58	[31]
III	Residual carbon and lignin removal, ash (inorganic noncombustible component) remaining.	370–575	16 - 20 (residual ash)	[24]
	Exothermic destruction of lignin	603	n/a	[8]
	Carbon oxidation, char (with silica) residue, tar formation	Above 350	n/a	[34]
	Thermal decomposition of lignin	370–600	26–31 (loss) 16 (Residual ash)	[31]

Table 3

Higher heating value, Proximate and Ultimate analysis of processed rice husk.

Rice husk processing	Proximate Analysis (%)				Ultimate Analysis (%)					HHV (MJ/kg)	Reference
	Volatile matter	Fixed Carbon	Moisture	Ash	C	H	N	O	S		
As received	n/a	n/a	n/a	n/a	37.05	8.80	11.06	35.03	n/a		[11]
Air dried rice husk	70.83	13.19	0.79	15.20	45.93	5.61	1.03	31.29	0.15		[33]
Compositions of biochar after carbonization											
Carbonization at 180 °C	n/a	n/a	n/a	n/a	40.63	5.37	0.69	29.31	0	16.17	[12]
Carbonization at 260 °C	n/a	n/a	n/a	n/a	45.32	4.72	0.22	23.88	0	17.79	[12]
Compositions of biochar after carbonization in controlled environment											
Carbonization at 220 °C, Ar inert environment	49.86	27.01	5.41	17.72	46.48	5.43	0.74	47.15	0.20	12.24	[44]
Carbonization at 220 °C, 21 % O_2 environment	22.37	34.98	5.46	37.19	64.58	6.01	1.46	27.86	0.09	12.78	[44]
Carbonization at 300 °C Ar inert environment	18.80	43.14	3.43	34.63	71.13	5.12	1.30	22.39	0.06	13.31	[44]
Torrefaction at 250 °C, inert environment, 60 min	40.50	29.89	n/a	29.61	64.62	5.57	0.91	28.84	0.06	14.35	[23]
Compositions of biochar after pretreatment, and carbonization											
260 W ultrasonic pretreatment, Carbonization at 260 °C	n/a	n/a	n/a	n/a	44.72	4.70	0.15	24.53	0	17.45	[12]
260 W ultrasonic pretreatment,10 % NaCl, Carbonization at 260 °C	n/a	n/a	n/a	n/a	40.95	4.70	0.10	25.80	0	16.02	[12]

Table 4

Chemical composition in rice husk ash.

Composition of rice husk ash after carbonization (without pretreatment)											
Pretreatment	Process Condition	SiO_2	CaO	Al_2O_3	K_2O	Na_2O	MgO	Fe_2O_3	MnO	P_2O_5	S	Reference
N.A	Above 800	92.3	0.8	0.2	1.4	0.1	0.4	0.1	0.2	0.7	n/a	[45]
Composition of rice husk ash after pretreatment and carbonization											
HCl leached	600 °C, 2 h.	99.58	0.04	0.17	0.02	n/a	0.02	0.03	n/a	0.11	0.02	[31]
H_2SO_4 leached	600 °C, 2 h.	99.08	0.05	0.61	0.02	n/a	0.04	0.02	0.01	0.13	0.05	[31]

Table 4.

Among the various pretreatment methods for rice husk, acid leaching is the most effective, followed by water soaking and then grinding [34]. Acid pretreatment is influenced by acid concentration, temperature, and duration of raw material pretreatment [8]. Acid pretreatment dissolves cellulose partially and most of the hemicellulose, with refractory lignin remaining. It has been shown that amorphous silica is formed at temperatures as high as 1000 °C with the use of strong acids to significantly leach out various impurities
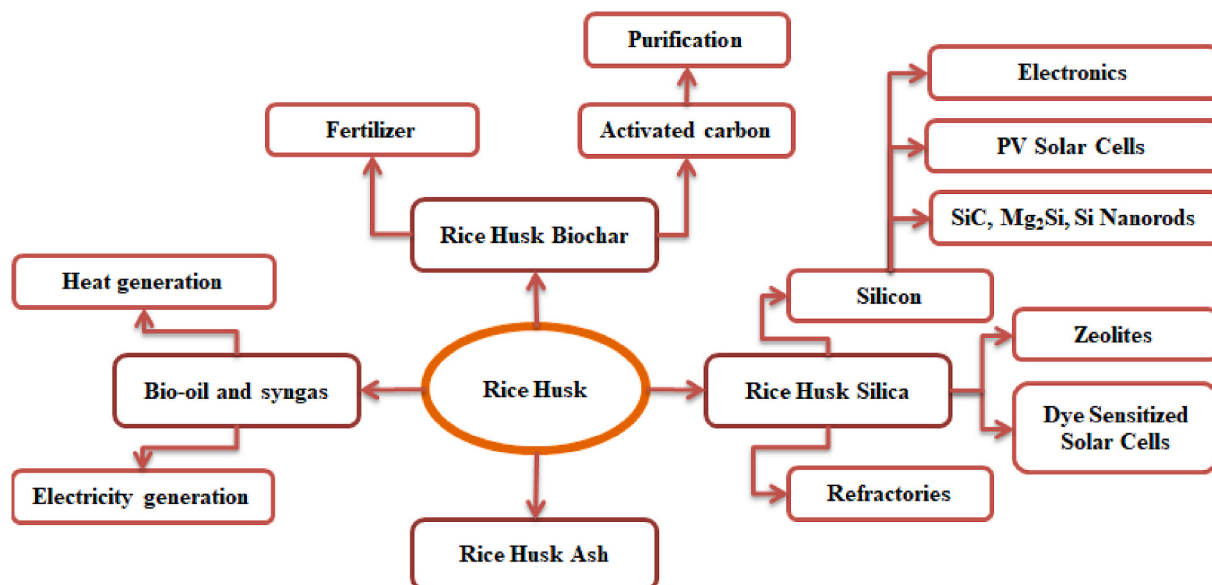
Fig. 1. Schematic of application of rice husk.

[11]. Hydrochloric acid (HCl) leaching is superior in removing metallic impurities compared to sulfuric acid (H_2SO_4) and nitric acid (HNO_3) [3].

The metallic impurities are mostly bound to the organic components (polysaccharide carboxyl groups) of rice husk, such as cellulose and hemicellulose. During acid pretreatment of rice husk, the polysaccharide carboxyl groups are hydrolyzed, producing levoglucosan and furfural monosaccharide. The carboxyl groups also form complexes in the acidic solution, which are discarded in the filtration and washing steps. Lignin, however, does not influence metallic impurities removal [15].

Acid leaching pretreatment before carbonization yields silica with a higher specific surface area than acid leaching post-treatment [11]. Acid-pretreated samples have enhanced sensitivity and reactivity to temperature, a more homogeneous structure, and an increase in activation energy [34]. Acid treatment also reduces carbon and other metal impurities, improving the brightness of the rice husk ash. During acid leaching of rice husk, the cellulose organic component of rice husk is leached out as smaller molecular weight compounds. This also leads to the blackening of the carbohydrates and removal of oxygen. Proteins within the husk are decomposed into amino acid monomers [38].

Acid leaching accelerates polycondensation of the siloxane bonds. Hence, acid leaching is relevant in removing metallic impurities. Acid leaching pretreatment leads to a longer time to achieve the decomposition temperature, indicating that acid hydrolysis decelerates thermal degradation at elevated temperatures. The deceleration of the thermal degradation process is due to the removal of metallic oxides and the weakening of the thermal degradation catalytic effect of organic compounds [34].

Silica surface melt caused by potassium impurity decreases the surface area and reactivity of the resulting rice husk ash [16], which also causes crystallization at lower temperatures [3]. Potassium oxide contained in RHA accelerates crystallization of amorphous silica into tridymite and cristobalite [3]. A slow heating rate can reduce the amount of unburnt carbon by oxidizing the carbon particles before the silica surface melt [38].

Simple thermal treatment of rice husk can yield 90 % silica purity [28]. Mineral acid solutions are used to pretreat rice husk to remove metal oxide impurities before carbonization [8]. An 8 wt% acid leaching at 120 °C, followed by grinding into 100 mesh sizes, is beneficial for metallic impurities removal and thermal decomposition of rice husk [34]. The oxidation of acid-leached samples is, however, sluggish at low temperatures [38].

Rice husk can also absorb amount of organic matter from the leaching agent during the leaching process which can distort the hydrogen bonds. This phenomenon leads to cell swelling. High acidity of leaching agents can also cause severe changes in physical biomass material properties. Acid leaching reduces the crystallinity as well as loosens the cell wall structure of the rice husk effectively releasing the metallic impurities from the cell structure [41].

Although strong acids are highly effective in removing metallic impurities, their release is, however, harmful to the environment and human health. The use of weak organic acids, such as citric acid, has been experimented with, yielding silica of purity above 99 % at temperatures around 800 °C. Additionally, the use of distilled or deionized water in rinsing/leaching metallic impurities is an alternative with less environmental impact. However, water leaching of rice husk carbonized at temperatures around 600 °C yields silica with a lower specific surface area, a narrow XRD peak with a smaller pore diameter, compared to acid-leached samples [3].

Hydrothermal carbonization has also been explored as a pretreatment step followed by carbonization. In the hydrothermal pretreatment step, a water medium is used as a substitute for acids, alkalis, and other chemicals to remove carbon dioxide, nitrogen oxides, and sulfur oxides within the rice husk feedstock. Hydrothermal pretreatment also has the advantage of enhanced reaction rate, cost reduction, and high-purity silica at industrial levels [11].
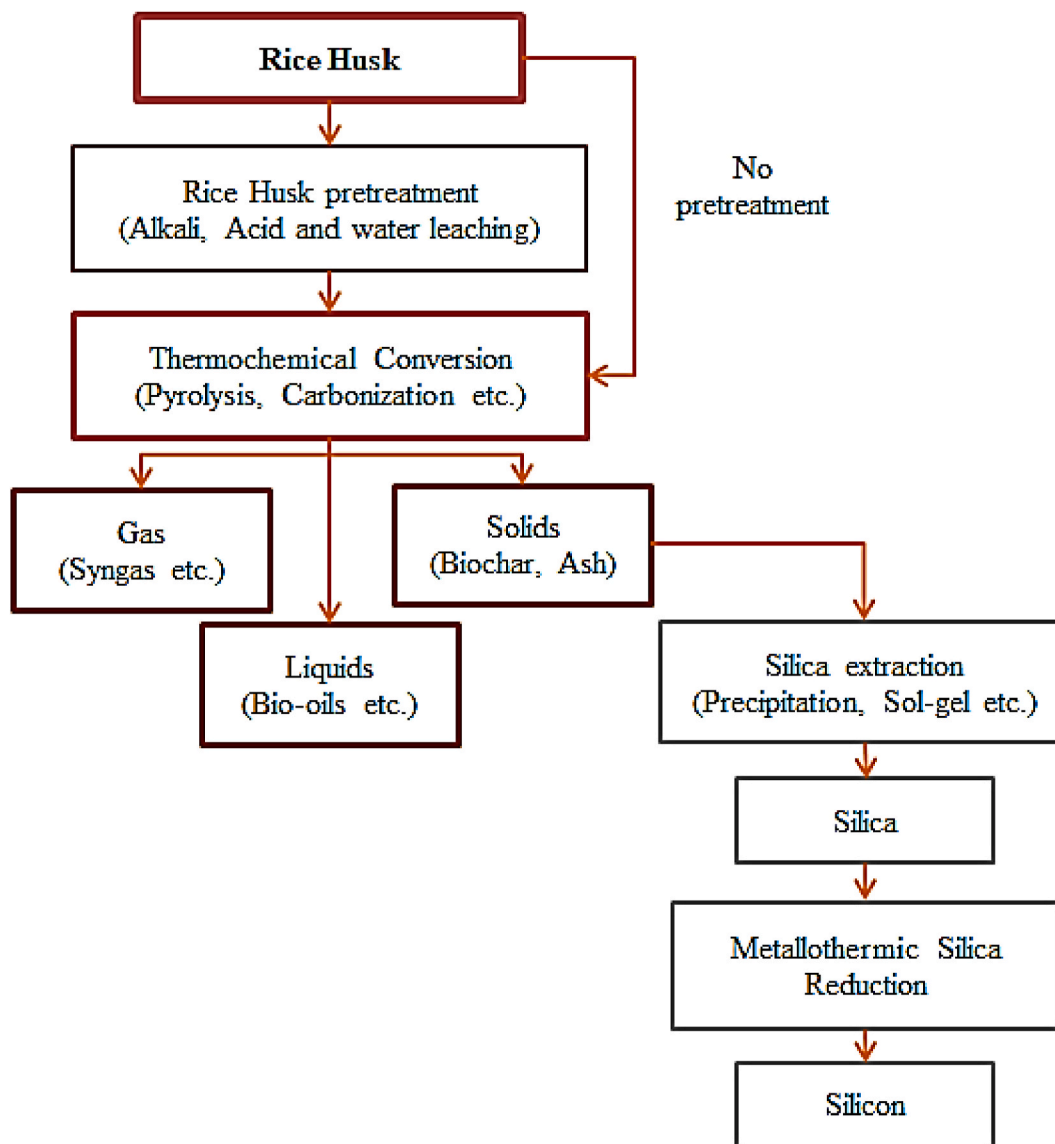
Fig. 2. Schematic diagram of the integrated silica and silicon synthesis from rice husk feedstock.

Other pretreatment such as alkali pretreatment is effective is reducing the ash content in rice husk by up to 85 %. Factors such as rice husk biomass to alkali ratio and alkaline solution concentration plays significant role in reducing the silica content of the rice husk ash – reducing the over ash content. As alkali concentration increases, silica removal also increases with decrease in calorific value of the alkali pretreated rice husk sample. This is an effective means of producing rice husk ash with high carbon content which can be used in the synthesis of materials such as activated carbon. Alkali such as NaOH react with the rice husk silica to form sodium silicate which is washed with water and separated in a subsequent solid-liquid separation stages [42].

Torrefaction is also used as a pretreatment method to remove oxygen within rice husk to enhance its fuel properties. The oxygen migrates into the gaseous and liquid products. The oxygen migration predominantly occurs via H_2O release followed by CO_2, and then CO. There is also carbon migration within the rice husk resulting in mass and energy increase [43].

2. Thermochemical conversion of rice husk approaches

Thermochemical biomass conversion approaches include gasification, co-firing, pyrolysis, liquefaction, hydrothermal electrolysis, carbonization, and combustion [46,47]. Thermochemical conversion leads to changes in physicochemical properties, such as elemental analysis, surface area, pore structure, and volume (including micropores, mesopores, and macropores) [22]. Thermochemical conversion approaches primarily yield gases and liquid intermediates, which are upgraded into valuable energy forms, including electricity, transportation fuels, and chemicals [47]. As shown in Fig. 3, the emissions occur as a result of the removal of

water, cellulose, hemicellulose, carbon and lignin as temperature increases. The products of thermochemical conversion approaches include biofuels, biochar, and value-added syngas [14].

Thermochemical treatments, such as gasification and pyrolysis, are promising in converting rice husk (RH) into useful products [43]. Gasification, known as an extension of pyrolysis, uses gasifying agents such as air, oxygen, and steam to enhance the yield of gaseous compounds from thermochemical conversion [47]. Biomass co-firing with coal is an efficient and clean thermochemical conversion approach for converting biomass to electricity at a low cost [47]. Thermochemical conversion of rice husk leads to the emission of greenhouse gases, including CO_2, CH_4, and H_2O, as well as CO, a criteria pollutant, and H_2 [33].

Yao et al. [33] investigated the emission of these gases during the pyrolysis of rice husk. Carbon monoxide (CO) release is high between 150 °C and 300 °C, which reduces and remains constant beyond 600 °C. The emission of CO is due to the cracking of carbonyl (C–O–C) and carboxyl (C=O) groups via the pyrolysis of cellulose and hemicellulose. There is also a release of CO_2 emissions between 200 °C and 400 °C and above 500 °C. The initial CO_2 release between 200 °C and 400 °C is due to the breaking of C=O bonds in hemicellulose. At temperatures above 500 °C, the CO_2 release is very low and results from the decomposition of lignin [33].

At temperatures between 100 °C and 500 °C, water is released as bulk water, bound water, and crystallization water in mineral substances. Above 500 °C, water from cracking or reaction of oxygen functional groups decreases slowly with increasing temperature. Methane is emitted around 180 °C, between 300 °C and 450 °C, and below 600 °C due to the cracking of methoxyl-O-CH_3 groups via pyrolysis of lignin. Hydrogen (H_2) gas is released due to the pyrolysis of cellulose and hemicellulose below 400 °C. Lignin decomposition above 400 °C generates relatively lower H_2 emissions [33].

2.1. Combustion/carbonization

Combustion is a simple thermochemical conversion process that occurs in the presence of air to generate heat and/or power [47]. The combustion of rice husk is an exothermic reaction that releases energy, which is useful for steam generation in energy production [9]. Carbonization, an extension of pyrolysis, yields mainly solid products through a slow heating rate thermochemical conversion process [47]. The combustion of rice husk generates fewer NOx and SOx emissions due to its lower combustion temperature and low sulfur content compared to fossil fuels [48].

Combustion, which produces carbon dioxide, is a better alternative to biomass decomposition, which produces methane with a high global warming potential. The combustion of a kilogram of rice husk generates between 13 and 16 MJ, which is comparable to the lower heating value of fossil fuels such as coal, peat, and lignite [11]. The properties of rice husk ash depend on the pretreatment and carbonization conditions [38]. When carbonized in an inert atmosphere, the organic compounds in rice husk decompose, yielding volatile compounds, CO_2, CO, water, and a solid residue of silica and carbon [49]. Under controlled carbonization, highly reactive and ultra-fine amorphous silica is produced [38]. Carbonization of rice husk at temperatures above 700 °C can lead to the formation of crystalline silica [49]. Schematic of the combustion process and the crystallize silica progression as temperature increases are shown in
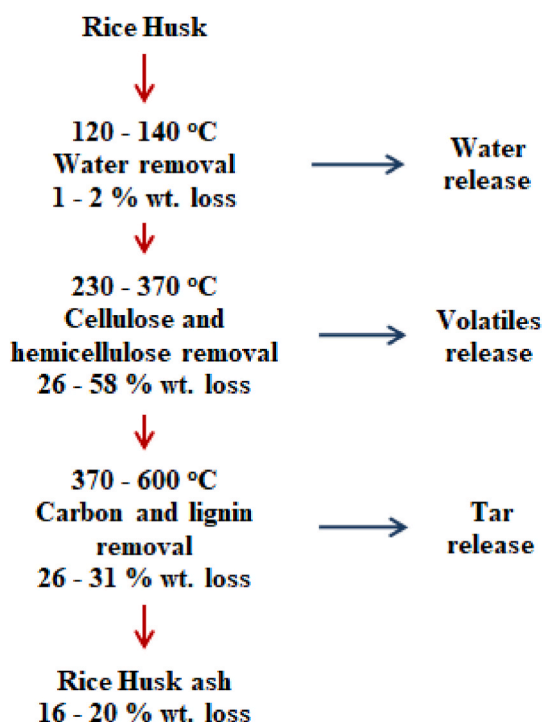

Rice Husk
↓
120 - 140 °C
Water removal
1 - 2 % wt. loss ⟶ **Water release**
↓
230 - 370 °C
Cellulose and hemicellulose removal
26 - 58 % wt. loss ⟶ **Volatiles release**
↓
370 - 600 °C
Carbon and lignin removal
26 - 31 % wt. loss ⟶ **Tar release**
↓
Rice Husk ash
16 - 20 % wt. loss

Fig. 3. Schematic of the decomposition of the components of rice husk and its temperature ranges.

Figs. 6 and 7.

Fluidized bed combustion, which has excellent heat and mass transfer characteristics, is suitable for rice husk combustion. In fluidized bed combustion, the turbulence due to fluidization is useful in breaking the rigid outer skeleton/shell of the rice husk, exposing the inner carbon content [11].

Carbonization of rice husk produces 14–20 % ash, which contains 82–95 % silica with trace amounts of metallic oxides [38,50]. The direct combustion of rice husk results in the formation of black particles due to unburnt carbon, which are trapped in silica surface melt due to the presence of potassium impurities [51]. Heating conditions, such as heating rate, carbonization temperature, and soaking time during pretreatment, affect the quality of rice husk ash [22].

Simple combustion/calcination of rice husk under controlled conditions is more economical and attractive compared to other methods [34]. The temperature and time of calcination/combustion are the primary factors determining the crystallinity of the produced silica material [8].

In the combustion method, oxygen within the biomass acts as an oxidizing agent, resulting in heat generation. Approximately 90 % of the rice husk is utilized for heat (energy) generation. The typical yield of silica from the combustion method (without alkali or acid pretreatment) is 95 wt%, with trace amounts of alkali oxides [10].

Rice husk combustion conditions, such as temperature and heating duration, affect the quality of the ash (whether amorphous or crystalline). Rice husk ash produced below 700 °C is generally amorphous, while ash produced above 800 °C is in the crystalline form. A low-temperature, longer heating duration or a higher temperature, shorter heating duration yields amorphous rice husk ash [52]. Completely burnt rice husk ash is typically grey to white in color, while partially burnt rice husk ash appears blackish due to the presence of unburnt carbon [28].

The use of fluidized bed technology with a rapid reaction time of 2 min consistently yields rice husk ash with less than 2 % carbon. The trapped carbon is exposed due to the breakage of the rigid ash skeleton caused by the turbulence of the fluidization system. Parameters such as fluidization velocity, reaction time, and combustion/fluidized bed temperature affect the quality of the rice husk ash. Temperatures and fluidization velocities between 500 °C and 700 °C, and 0.30 and 0.40 m/s, are most suitable for amorphous silica extraction. Crystalline silica forms, such as quartz, can form through the fluidization method of silica synthesis due to bed elutriation. However, cristobalites tend to form at fluidization velocities between 0.40 and 0.50 m/s [36].

2.2. Liquefaction

Liquefaction, also known as hydrothermal liquefaction, is a thermochemical conversion approach that involves the use of water at high temperatures as a catalyst and reactant to disintegrate and reform biomass material into hydrocarbons. Wet biomass samples can be liquefied directly, eliminating the drying unit operation step, which translates into reduced energy use [47]. Liquefaction is the most environmentally friendly approach among the thermochemical conversion methods, with less energy use.

The liquefaction reaction is catalyzed using an alkaline catalyst, such as potassium hydroxide and sodium carbonate, and is a decomposition reaction that consists of dehydration, alcohol solvent vaporization, and alcoholysis of biomass. The use of an alcohol solvent as the reaction medium at supercritical operation conditions also enhances liquefaction. The supercritical solvent exhibits both gaseous and aqueous properties, including low viscosity (similar to gases) and high density (similar to liquids), as well as higher diffusivity to enhance chemical reactions [46].

Echaroj et al. [46] produced biofuel from rice husk feedstock using graphene oxide as a catalyst through liquefaction. The optimum biofuel production conditions were 298 °C supercritical ethanol liquefaction, 60 min of reaction time, and 3.4 g of SO_4 (1.5)/graphene oxide catalyst, resulting in a biofuel yield of 51.8 %. The higher heating value (HHV) of the produced biofuel was 30.15 MJ/kg, with an elemental composition of 61.2 % carbon, 9.96 % hydrogen, 24.7 % oxygen, and 4.14 % nitrogen.

2.3. Torrefaction

At temperatures between 200 °C and 300 °C, a slow pyrolysis of biomass occurs, known as torrefaction. Torrefaction is primarily used as a pretreatment procedure to enhance the physicochemical properties of thermochemical conversion of various biomass materials [23].

Zhao et al. [44] investigated the effects of torrefaction in oxidative and inert atmospheres. Torrefaction in inert conditions increased the fixed carbon content and heating value in the upgraded rice husk samples. Among the torrefaction conditions in inert and oxidative (0, 6, 10, and 21 vol% oxygen) atmospheres and temperatures (493, 543, and 573 K), the 6 vol% oxygen at 573 K condition had the optimum surface behaviors and hydrophobicity.

2.4. Hydrothermal process

Hydrothermal processing involves the use of a single or heterogeneous phase in aqueous media, such as water, at elevated temperatures and autogenous pressure [30]. The hydrothermal synthesis method utilizes subcritical water (at a critical point of 100–374 °C) as the reacting and extraction medium, which is more environmentally friendly, resulting in less pollution and energy use [32].

The hydrothermal carbonization (HTC) process involves three stages: solubilization (at 120 °C), hydrolysis (between 140 °C and 180 °C), and carbonization (between 200 °C and 260 °C). However, the temperature for the carbonization stage is not well-defined. Oxidants (H_2O_2) and catalysts (acids, alkaline, and eutectic solvents) are used in the HTC process [30]. Schematic of the hydrothermal

process is shown in Fig. 4.

Subcritical water has a low dielectric constant, low viscosity, and high solubility of organic substances [32]. The electronic properties and surface chemistry can be easily controlled without changing the morphology by additional thermal treatment [2]. In the hydrothermal process, the dielectric constant of water decreases, and the hydrogen bonds weaken, increasing the ionization constant [30]. The hydrothermal process is characterized by the dissolution of gases such as carbon dioxide, sulfur oxide, and nitrogen oxide in the water medium, enhanced reaction rates, and versatile chemistry [3].

Draszewski et al. [53] used subcritical water to hydrolyze rice husk at 180 °C, 220 °C, and 260 °C as the raw material for silica synthesis. The TGA thermogram showed a maximum weight loss of 13 % until 600 °C, indicating the composition and thermal stability of the extracted silica. The broad XRD peak at $2\theta = 22°$ confirmed the presence of amorphous silica. The FTIR spectrum indicated siloxane bonds at 1070-1090 cm^{-1}.

Under high temperature, pressure, and acidic/basic medium, the organic components of rice husk are decomposed, and the metallic impurities are solubilized. However, the hydrothermal process requires a carbonization/incineration final step to eliminate other unwanted impurities fully and synthesize highly pure silica [30]. The carbon yield in hydrothermal carbonization (HTC) is about 70–80 %, which is generally higher than pyrolysis. Wet biomass can be processed directly in a hydrothermal carbonization process without drying [2].

In Tolba et al. [32] research, hydrothermally synthesized amorphous nanosilica with an 81 % yield was used as a reusable adsorbent for organic pollutants. The synthesized nanosilica had particle sizes of 10–50 nm (with an average of 30 nm) and a methylene blue dye (10 ppm) removal efficiency of 65 % within the first minute. The regeneration of the used nanosilica at 450 °C further enhanced the removal efficiency (which was linearly dependent on the number of successive absorption-regeneration cycles).

Akter et al. [54] conducted research on the subcritical water extraction of tannery sludges at 240 °C and 540 min, supplemented with silica from rice husk and $Ca(OH)_2$ to synthesize tobermorite. The synthesized tobermorite was used to extract heavy metals such as chromium, copper, magnesium, and lead. The tobermorite successfully reduced the concentration of chromium from a very high risk category of 11.24 mg/L Cr to 1.6 mg/L. The rice husk silica was synthesized at 650 °C for 2 h after the raw rice husk was cleaned with Milli-Q and dried at 105 °C for 24 h.

Z. Xu et al. [12] investigated the influence of NaCl on the hydrothermal carbonization of rice husk, using ultrasonic pretreatment. It was observed that NaCl improves hydrolysis, dehydration, and decarboxylation during the hydrothermal carbonization of rice husk samples. NaCl solubilized the organic matter in rice husk (RH). NaCl also enhanced the polymerization of lignin components into monomers while removing hemicellulose from the rice husk during the hydrothermal process. This led to cracks on the hydrochar surface. Increasing the hydrothermal temperature decreased the nitrogen (N), oxygen (O), and hydrogen (H) content, indicating the breakage of the cellulose and hemicellulose network in the rice husk.

There are two main hydrothermal processes: low-temperature and high-temperature hydrothermal processes. The high-temperature hydrothermal process utilizes high temperatures (>243 °C) and pressures (>3 MPa) to leach out solution oxide impurities and degrade organic compounds in rice husk. In contrast, the low-temperature hydrothermal process employs lower temperatures (<240 °C), which hardly affect the local silicate structures. The low-temperature hydrothermal process preserves the Q4 (silicon oxygen tetrahedral framework, SiO_4 or $(Si(OSi)_4)$), Q3 (silanol groups, $(O)Si(OSi)_3$), and Q2 (silanediol, $(OH)_2Si(OSi)_2$) units. The Q3 silanol unit is related to the hydroxyl functional group (C-O-H) found in alcohols [3]. Hydrothermal carbonization yields carbon materials with several functional groups on their surface, which are important for numerous applications [2].

2.5. Pyrolysis

Pyrolysis, which is often the primary step in most thermochemical conversion processes, leads to the production of three different product phases [47]. Biomass pyrolysis is a thermochemical decomposition process that occurs in an oxygen-deficient environment at elevated temperatures [2]. The pyrolysis process is a thermochemical process that transforms biobased/carbonaceous materials into useful products, such as oils, biochar, and gas, by releasing moisture and volatile content [22].

Biomass pyrolysis products are mainly carbon-rich charred residues, liquid products, and gases [2]. The char is used as a precursor material for the synthesis of silicon nitride and silicon carbide [3]. Pyrolysis of agricultural waste (rice husk) yields ashes, active carbons, and biochar, which are influenced by the particle size of the precursor material, heating rate, and temperature [22]. The distribution of cellulose, hemicellulose, and lignin influences the nature of pyrolysis products [29].

The stability of biochar from rice husk pyrolysis is determined by particle size, silicon protection, and aromatic structures. At temperatures below 250 °C, dehydration of biochar occurs, and carbon and silicon integrate, while silicic acid polymerizes between 250 °C and 350 °C. Additionally, the silicon components from the internal biochar tissues become exposed due to the cracking of carbon components. At higher temperatures, between 500 °C and 700 °C, the carbon aromatizes, and the silicon crystallizes [14]. The
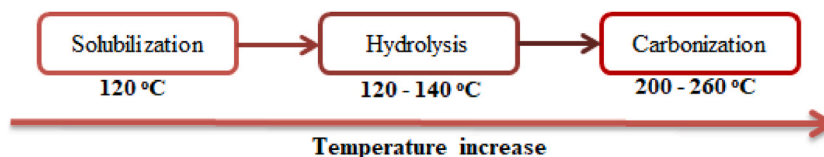
Fig. 4. Schematic of the hydrothermal process.

schematic of the pyrolysis process is shown in Fig. 5.

Pyrolysis can be subdivided into slow or fast pyrolysis based on the operating temperature and residence time. Fast pyrolysis, which has a dominant liquid product, occurs at moderate temperatures and very short/low residence times. In contrast, slow pyrolysis, which primarily produces solid (charcoal), occurs at longer residence times, low heating rates, and moderate temperatures [47].

As temperature increases, particle size decreases, solids yield decreases, and gases yield increases, resulting in an increase in crystallinity of inorganics and a reduction in particle reactivity [22]. Increasing the pyrolysis temperature results in the removal of non-carbonaceous gases and tarry hydrocarbons trapped by the free interstices due to irregular arrangements [3]. Volatiles such as hydrogen, carbon dioxide, and carbon monoxide are released during the pyrolysis process [9]. Temperature increases lead to decreases in volatile matter, secondary decomposition of charcoal residue, and therefore yield high-quality ash [22].

Steam and suitable oxidizing gas activation are required to activate the material by removing trapped tarry and volatile substances [3]. Bio-oils and syngas can be extracted from rice husk pyrolysis processes. Silica and high specific surface area activated carbon can be extracted from biochar produced by rice husk pyrolysis. Biochar from rice husk pyrolysis can be used in soil remediation, silicon materials production, and pollutant removal [14].

Pyrolysis of acid-leached rice husk at 800 °C for 1 h is more efficient in silica production compared to water-rinsed rice husk pyrolyzed at 800 °C for 8 h, which still contains carbon residue. Pyrolysis of untreated rice husk at temperatures above 800 °C leads to the removal of carbon residue but results in the production of crystalline silica [2]. Thermal pyrolysis of pretreated rice husk provides a simple and cost-effective synthesis route compared to other methods, such as the precipitation method [19].

Glushankova et al. [24] pyrolyzed rice husk at 475 °C, yielding 50 wt% crude bio-oil. However, the pyrolyzed bio-oil is more acidic (pH = 3.2) compared to diesel oil (pH = 7.8). Adeniyi et al. [29] modeled and simulated the pyrolysis of rice husk between temperatures of 400 °C and 600 °C. The pyrolysis oil yield decreased from 44.2 % at 400 °C to 41 % at 500 °C and finally to 32.9 % at 600 °C. This decrease is due to the intense cracking of larger polymer molecules as the temperature increases. The pyrolysis gas yield increased from 17.1 % at 400 °C to 25.2 % at 600 °C. The char yield (consisting of carbon and silica) increased from 38.7 % to 41.9 % between 400 °C and 600 °C. The oil product from the pyrolysis process contains aldehydes, pyrolytic water at 600 °C, the predicted oil composition consisted of 84.7 % acidic organic compounds, 7.42 % aldehyde, and 7.9 % pyrolytic water.

Gu et al. [19] investigated the effect of various parameters, such as hydrochloric acid concentration (wt%), hydrolysis temperature (°C), hydrolysis time (h), ratio of rice husk (RH) to acid (g:ml), and pyrolysis temperature (°C), on the synthesis of photosensitive nanosilica using an orthogonal experimental design. The optimum process parameters for silica production (99.92 % silica purity, 8–10 nm average particle size) were found to be 8 wt% HCl concentration, 120 °C hydrolysis temperature, 4 h hydrolysis time, 1 g RH: 10 ml acid solution, 610 °C pyrolysis temperature, and particle size between 250 and 420 μm. The optimum process parameters for whiteness (91.03 %) were 8 wt% HCl concentration, 120 °C hydrolysis temperature, 2 h hydrolysis time, 1 g RH: 6 ml acid solution, and 650 °C pyrolysis temperature. The significance of the process parameters in decreasing order was pyrolysis temperature > hydrolysis temperature > ratio of RH to acid > hydrolysis time > hydrochloric acid concentration. A maximum whiteness of 94.18 % and silica content of 99.92 % were obtained for particle sizes between 250 and 420 μm.

2.5.1. Kinetics of pyrolysis

The kinetics of pyrolysis can be understood by analyzing the TGA thermogram, which shows that pyrolysis of rice husk occurs in four stages: dehydration (110–120 °C), transition (120–210 °C), decomposition (210–470 °C), and carbonization (above 470 °C). The dehydration stage involves moisture loss. The decomposition stage involves the loss of volatile compounds, decomposition of aromatic compounds, removal of hydrogen bonds, and extraction of hemicellulose and cellulose [19].

Pyrolysis involves two main steps. Firstly, lignin and cellulose undergo depolymerization or decomposition into organic materials with small molecular weights, releasing intermediates and gaseous volatile compounds from lignin and cellulose constituents. The decomposition of cellulose and lignin overlap in the first stage; however, lignin requires higher activation energy due to its difficulty in decomposition compared to cellulose. Secondly, the intermediates (residual organic matter) are further pyrolyzed to form tar and char (consisting of silica and carbon) [3].

2.6. Kinetics model of thermochemical conversion

In the research by Gu et al. [34], the kinetics of rice husk silica synthesis under various pretreatments was examined. The Flynn-Wall-Ozawa (FWO) method was used to derive kinetic parameters such as the correlation coefficient and activation energy. The
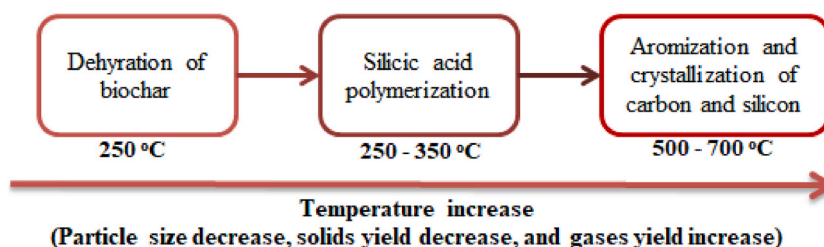

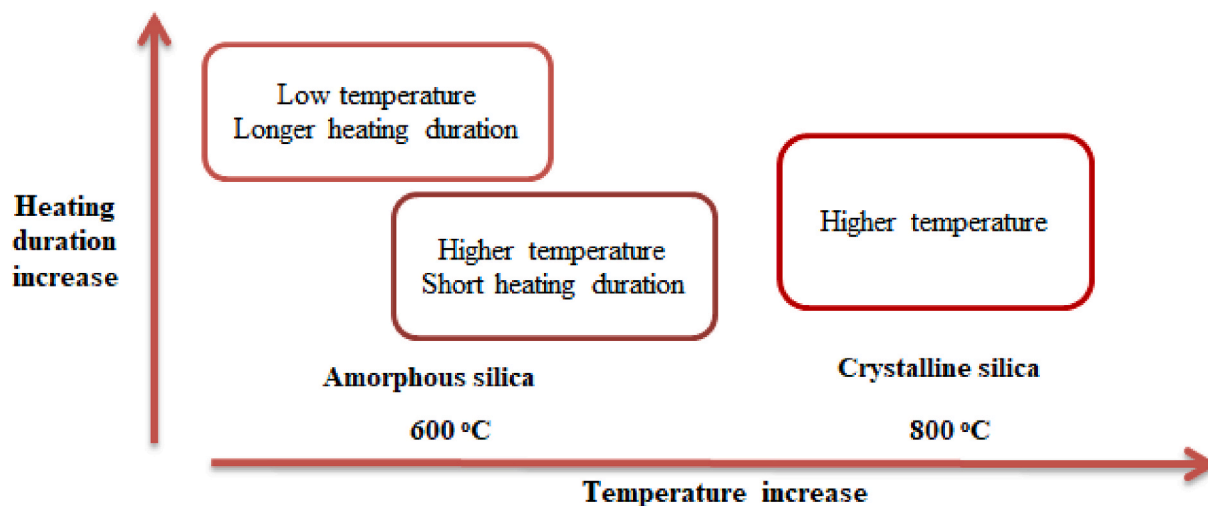**Fig. 5.** Schematic of the pyrolysis process.

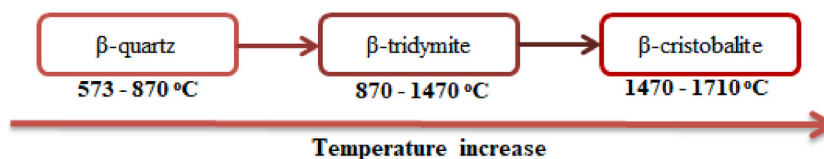**Fig. 6.** Schematic of the carbonization process.

Fig. 7. Schematic of crystallize silica progression as temperature increase from quartz to cristobalite.

FWO kinetic method is an isoconversional technique that relates activation energy to temperature and heating rate at constant conversion. Additionally, the FWO method is model-free. The calculated activation energy ranged from 90 to 156 kJ/mol.

J. Zou et al. [23] explored the use of the Generalized Logistic Mixture Model (GLMM) and the Distributed Activation Energy Model (DAEM) to examine the kinetics of torrefied rice husk pyrolysis. The GLMM was shown to be effective in deconvoluting overlapping subprocesses, while the DAEM enabled the estimation of various activation energies of the deconvoluted subprocesses in biomass pyrolysis. The pyrolysis process of torrefied rice husk was deconvoluted into two subprocesses: the thermal decomposition of pseudo-cellulose and pseudo-lignin. Typically, most biomass feedstock decomposition includes an additional subprocess of thermal decomposition of pseudo-hemicellulose.

The Lumped and Distributed Kinetic model is a typical lignocellulosic pyrolysis kinetic model based on different reaction pathways. The Lumped Kinetic model considers materials as single (lumped) homogeneous materials or various single homogeneous materials, such as tar, char, and gas. In contrast, the Distributed Kinetic model (also referred to as the Distributed Activation Energy Model, DAEM) is associated with different reaction activation energies due to several parallel reactions from the pyrolysis of various components (e.g., lignocellulose) of the material [23].

3. Silica

The two oxides of silicon are silicon dioxide (silica, SiO_2) and silicon monoxide (SiO) [55]. Silicon bonds to four oxygen atoms, with each oxygen atom bonding to two silicon atoms [2]. Silica, with the general formula SiO_2, is a polymeric material composed of silicic acid, constituting an SiO_4 tetrahedral structure [56]. The SiO_4 tetrahedral shape of silica forms hexagonal 6-membered rings, with each oxygen bonding to two silicon atoms (siloxane bonds) [17].

Silica is a white, fluffy, odorless, powdered solid material with a melting point of 1700 °C–1740 °C, a boiling point of 2230 °C, a density of 2–3 g/cm^3, and a specific gravity of 2.650 at 20 °C [2,9]. Silica occurs naturally in three crystalline forms: quartz (hexagonal), cristobalite (white), and tridymite (hexagonal) [9]. Mineral quartz is primarily found in hydrothermal bodies or pegmatites [55].

Silica undergoes hydration and dehydration within the Earth's biosphere through a reversible, pH-dependent hydrolysis and condensation reaction [17]. Silica, the most abundant oxide component of the Earth's crust [17,57], occurs naturally in crystalline form (crystalline quartz), whereas synthetic silica is mostly amorphous (synthetic amorphous silica nanoparticles) [17].

The crystalline silica forms in nature are quartz, tridymite, and cristobalite [55]. Although silica is abundant in the Earth's crust, its purification is highly energy-intensive [9]. The most stable silica phase is quartz, with a boiling point of 2275 °C and a melting point of 1726 °C [55].

Silica in nature exists in crystalline form, whereas synthetically produced silica is amorphous [56]. Synthetic amorphous silica

nanoparticles (SASNs) are the most abundant synthetic nanoparticles on Earth [17]. The precursor material sources of synthetic amorphous silica include silane reagents and silicate solutions [56].

Rice husk silica is present in amorphous form as opal silica; however, through thermal treatment, the rice husk silica is converted to crystalline form [9]. The formation of amorphous silica instead of crystalline silica is due to the low free energy and heat of crystallization of silica, resulting from the high flexibility of the siloxane bonds [17].

The nature of synthesized silica is highly dependent on the synthesis route and environmental factors [17]. Under controlled calcination conditions and lower temperatures, amorphous silica with high surface area, fine particles, and reactivity is produced [18].

The conventional industrial method for silica synthesis involves the use of sodium silicate, obtained by melting quartz sand and sodium carbonate at 1300 °C [8]. Silica obtained from the carbonization of rice husk at different temperatures and times has varying ash components [57]. Carbonization between 600 °C and 1000 °C primarily yields amorphous silica, whereas higher temperatures yield crystalline silica [31].

Silica is the main inorganic constituent of rice husk, with ultrafine particles and suitable particle diameter [28]. Rice husk ash is categorized into amorphous, crystalline, and partially crystalline forms based on temperature and time. Rice husk ash from quick open-air burning contains high amounts of carbon. Crystallized silica is produced through slow burning of rice husk at 600 °C, whereas amorphous silica (considered reactive) is obtained by burning rice husk at temperatures around 500 °C.The suitable temperature for amorphous silica production is between 500 °C and 800 °C; higher temperatures yield crystallized silica and can cause particle agglomeration [13].

Temperature, time, and other factors play a crucial role in determining the structure and properties of rice husk silica. To achieve higher silica purity, metallic impurities must be removed. Processes for removing impurities include acid leaching before or after thermal treatment using acid solutions such as HCl, H_2SO_4, HNO_3, and H_3PO_4, as well as alkaline solutions like NH_4OH and $NaOH$ [14].

Chemicals used to leach impurities from rice husk/rice husk silica include HF, H_2SO_4, HI, H_3PO_4, HCl, and $C_6H_8O_7$. Hydrochloric acid (HCl) is the most effective acid, yielding 91–99 % silica purity. Citric acid, unlike mineral acids like HCl, H_3PO_4, H_2SO_4, and HF, is more environmentally friendly. The carbonyl cluster in citric acid binds with metal impurities in the rice husk to form complex compounds [35].

Using citric acid to leach metal oxide impurities provides a less toxic and cheaper pretreatment option [8]. The optical properties of rice husk ash are influenced by colored metal oxide impurities, but more significantly by the color of carbon produced during rice husk carbonization. Brightness, used to measure the whiteness of rice husk ash/silica, is the percentage of light reflected at a 457 nm wavelength. Yellowness is the difference between the percentage of light reflectance at 457 and 570 nm wavelengths [38].

3.1. Factors that affect silica synthesis/extraction from rice husk

Several factors influence silica synthesis from rice husk, including rice husk particle size, pretreatment conditions, and calcination conditions of the rice husk raw material. Particle size affects the internal heating rate of the rice husk samples and the volatiles precipitation rate, altering the pyrolysis behavior of the rice husk biomass [34].

Decreasing particle sizes increases the reactivity of the particles with acid during the acid leaching pretreatment phase, leading to the removal of more metallic impurities. Smaller particle sizes also enhance rapid heat absorption and thermal decomposition in air due to decreased devolatilization temperature and time. However, excessively fine particles can cause local overheating of the samples, leading to a large temperature gradient surrounding the sample, which decreases the reaction rate and influences the thermal decomposition equilibrium. Reducing particle sizes through grinding can improve silica purity by approximately 1 % [34].

The synthesis of silica from rice husk is influenced by several factors, including acid treatment, annealing temperature, and extraction route. These factors affect the particle size, surface area, and purity of the extracted silica. The purity of silica increases with the number of chemical treatment steps. Appropriate treatment of rice husk or rice husk ash with alkali or acid can increase the purity from 95 % (using only the combustion method) to over 99 % [10].

Gu et al. [34] observed that even low acid concentrations (<4 %) dissolve hemicellulose, and acid concentrations below 6 % do not affect the thermal decomposition rate. Acid concentrations above 8 % have no significant effect on the decomposition of rice husk. The decomposition of hemicellulose into tar and low-activity char formation results in narrower TGA stages temperature ranges compared to acid-pretreated samples.

Acid leaching is more effective than water rinsing in achieving higher silica purity [2]. The use of ionic liquids, such as 1-butyl-3--methylimidazolium hydrogen sulfate, is also effective in dissolving lignocellulose in rice husk, improving silica purity [15]. Nitric acid pretreatment of rice husk and calcination at 600 °C yield a white, amorphous, and highly pure silica (98.5 %) [38].

Pyrolysis at high temperatures and longer durations leads to the elimination of carbon residue, resulting in highly pure silica [2]. Krishnarao et al. [58] observed that bright white ash is generated at 700 °C for acid-treated rice husk; however, the heating rate had no effect on the formation of white ash. Slow heating of rice husk results in silica ash with fewer black particles due to enhanced oxidation of carbon present.

Chandrasekhar et al. [59] found that silica from acid-pretreated rice husk is mostly whiter than that from untreated rice husk. The whiteness of synthesized rice husk silica increased with temperature, reaching 57.0 % whiteness at 850 °C for 2 h. The whiteness of already charred rice husk was highest at 40.3 % at 800 °C for 2 h of calcination.

Amorphous rice husk silica is produced by calcining rice husk at temperatures below 800 °C, whereas crystalline silica is produced at temperatures above 900 °C. At temperatures above 700 °C during rice husk silica synthesis, an aggregation process occurs due to condensation of silanol groups (Si-OH) [3].

The transition from pure amorphous silica to crystalline silica takes place at temperatures above 1000 °C; however, the presence of various alkali oxides forms fluxes that reduce the transition temperature below 1000 °C [52]. Various literature data on the properties of synthesized rice husk silica are shown in Table 6.

3.2. Rice husk silica extraction methods

The conventional method for silica synthesis involves smelting quartz with sodium carbonate at 1300 °C [60]. However, this process is energy-intensive, toxic, and environmentally unfriendly [3]. Rice husk, an agricultural waste, offers a cheap, non-toxic, and environmentally friendly precursor material for silica synthesis [7,8].

Several methods are employed for silica extraction from rice husk, including sol-gel processing [10,34], chemical methods, combustion methods [56,61], microemulsion processing, chemical vapor deposition, hydrothermal techniques, and plasma synthesis [3]. Other methods include thermal pyrolysis, chemical precipitation [21,30,32], biotransformation [2,13,32], vapor phase reaction (VPR), thermal decomposition technique (TDT) [30], thermochemical redox reaction [62], and NH_4F dissolution (a mixture of ammonia and HF) [21,34].

Different silica synthesis methods from rice husk have distinct effects on the structure and morphology of the synthesized silica [30]. Table 5 presents various rice husk silica synthesis processes and their outputs.

3.2.1. Biotransformation

A wide range of biological organisms, including sponges, mollusks, protozoa, and higher plants, produce silica in the form of amorphous hydrated silica ($SiO_2 \cdot nH_2O$). Silica production by these organisms occurs under saturated silicic acid solutions in aqueous environments at temperatures between 4 °C and 40 °C [2].

The fungus Fusarium oxysporum has been used to transform naturally occurring amorphous biosilica in rice husk into high-crystalline, quasi-spherical silica nanoparticles with diameters of 2–8 nm [2,13]. The use of Californian red worms in silica synthesis from rice husk feedstock through a bio-digestion process has also been explored [30].

The white rot fungus, Cyathus, has been employed in the microbial fermentation of rice over 60 days, followed by a subsequent carbonization step at temperatures around 450 °C. This process yields silica with smaller sieve fractions compared to silica synthesized from untreated rice husk. Californian red worms are also effective in digesting rice husk; the excreted humus is then neutralized (using $CaCO_3$) and calcined at temperatures between 500 °C and 700 °C [11].
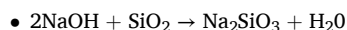
Although the use of biological organisms is more natural, it is typically explored as a pretreatment step followed by a carbonization/calcination step. Biotransformation is also time-consuming compared to other synthesis methods and requires suitable temperature conditions for optimal operation of the biological organisms [32].

3.2.2. Precipitation method

The precipitation method is a physico-chemical process involving alkali solubilization and final acid precipitation [30]. Silica in rice husk ash reacts with an alkali, such as sodium hydroxide (NaOH), to form sodium silicate [1,9,13]. This reaction occurs at temperatures between 180 °C and 200 °C under 6–8 atm pressure [9]. However, rice husk ash obtained from rice husk carbonized in a controlled environment requires a significantly lower reaction temperature [9].

The transparent, viscous sodium silicate solution, obtained after filtering the slurry (digested residue ash, free NaOH, and water), is then precipitated with an acid to form silica [9,30]. Acid addition is done slowly in a controlled process within a neutralizer at atmospheric pressure and 80–90 °C [9]. The resulting wet silica is filtered, washed, and dried to obtain high-purity silica [9].

Alkali solubilization.

- $2NaOH + SiO_2 \rightarrow Na_2SiO_3 + H_2O$

Acid precipitation.

- $Na_2SiO_3 + H_2SO_4 \rightarrow SiO_2 + Na_2SO_4 + H_2O$
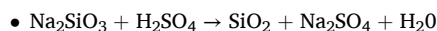
Table 5
Various synthesis method of rice husk silica.

Rice husk silica synthesis				
Treatment	Reagent	Process condition	Silica properties	references
Pretreatment	15 v/v % H_2SO_4, 100 °C, 6 h	600 °C for 5 min.	235–250 m²/g surface area, 0.9–10 μm average particle, 99.9 % pure silica	[4]
Precipitation	1 N NaOH, 1 N HCl	600–700 °C for 6 h 5 °C/min heating rate	90–98 % pure silica	[20]
Pretreatment	15 v/v % H_2SO_4, 100 °C, 6 h	600–650 °C	>99 % pure silica	[8]
Pretreatment	0.5 HCl, 60 °C, 30 min	600 °C for 2 h	99 % pure silica	[31]
Pretreatment	0.5H_2SO_4,60 °C, 30 min	600 °C for 2 h	99 % pure silica	[31]
Pretreatment	72 % conc. H_2SO_4	800 °C, for 48 h	99.6 % pure silica	[15]
Pretreatment	HCl	550 °C	Siloxane and silanol functional group, 93.08 %. pure silica	[62]

Table 6
Properties of extracted rice husk silica.

Process	BET Surface Area (m^2/g)	Pore Volume (m^3/g)	Particle sizes (nm)	SiO_2 yield (%)	Reference
carbonization at 600 °C	220	0.26	n/a	97.2	[77]
acid leached pretreatment, 600 °C carbonization	353	0.52	n/a	99.8	[77]

- $Na_2SiO_3 + HNO_3 \rightarrow SiO_2 + Na_2NO_3 + H_2O$
- $Na_2SiO_3 + 2HCl \rightarrow SiO_2 + 2NaCl + H_2O$
- $3Na_2SiO_3 + 2H_3PO_4 \rightarrow 3SiO_2 + 2Na_3PO_4 + 3H_2O$

The use of NaOH in silica extraction from rice husk ash (RHA) is less energy-intensive and offers economic and environmental advantages [56]. Although silica production via chemical precipitation yields highly pure silica, it is characterized by high reagent consumption, complex processes, and high costs [19,32].

The properties of precipitated silica, such as particle size, morphology, specific surface area, and porosity, are influenced by various factors, including modes of washing and drying, surfactant addition, pH, synthesis temperature, and time [63].

3.2.3. Sol-gel method

The sol-gel synthesis method has been shown to yield high-purity silica (approximately 99.9 %) [4]. This method involves converting a sol of silicon alkoxide, halide, or sodium silicate into a polymeric gel. Hydrolysis and condensation occur simultaneously in the sol-gel process. Conditions such as gel growth restriction lead to silica precipitation, which involves the coagulation and precipitation of the silica solution [56].

3.3. Characterization of rice husk silica

Among the techniques used in characterizing silica are XRD, XRF, SEM, FT-IR and BET.

3.3.1. X-ray diffraction (XRD)

X-ray diffraction (XRD) is a quantitative diffractometric technique [64]. XRD is used to analyze the crystal properties, chemical composition, and phases of materials [12,65,66]. This technique can determine whether a material is crystalline or amorphous, with a broad peak indicating amorphous [30]. A broad peak at Bragg 2θ at 22° corresponds to amorphous silica [30,67].

In an XRD diffractogram, a broad, smooth hump peak between 15° and 35° (2θ) indicates the conversion of crystalline cellulose structure to a random, disordered structure, characteristic of amorphous materials [11]. The amorphous diffractogram peak also indicates the adsorption properties of the rice husk material. As temperature increases, the peak intensity also increases around 22° (2θ), indicating the presence of crystalline material. This outlines the crystal structure organization, resulting in reduced surface area and decreased adsorption properties [11].

Three crystalline phases (quartz, tridymite, and cristobalite) are formed as the temperature increases from 550 °C to 1700 °C. Fig. 8 a, b shows the XRD diffractogram indicating the characteristic peaks of amorphous silica and the various crystalline phases.

3.3.2. Scanning electron microscopy (SEM)

Scanning electron microscopy (SEM) is a technique used to analyze the morphology and porous nature of materials [12,54].
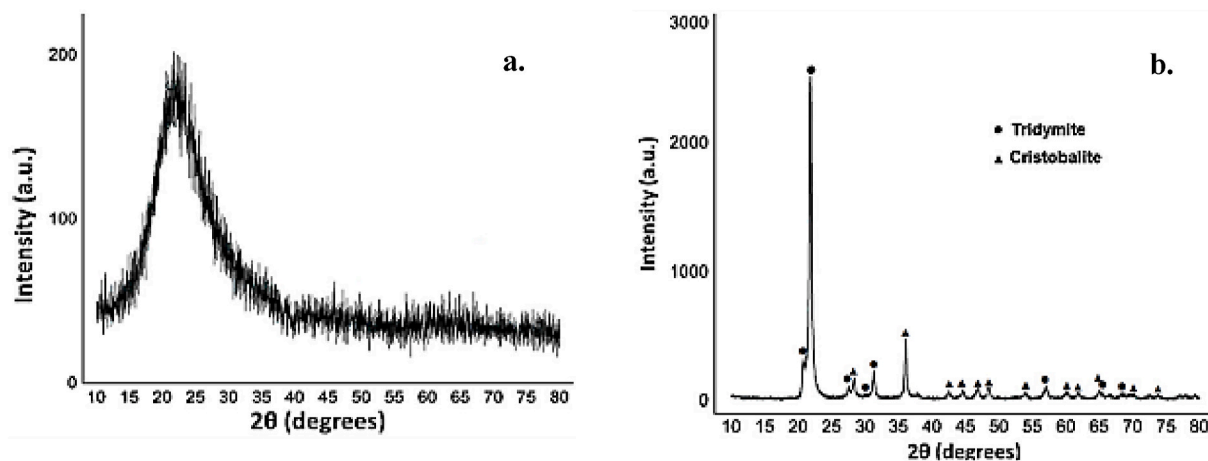

Fig. 8. XRD diffractogram of a. amorphous rice husk silica b. crystalline rice husk silica [68].

Additionally, SEM is employed to examine the structure of materials [65]. Fig. 9 displays an SEM micrograph of as-received rice husk, showcasing the lateral layers on the rice husk surface.

Field-Emission Scanning Electron Microscopy (FE-SEM) provides detailed analysis of a material's elemental data and topography at various magnifications, ranging from ×10 to x300,000 [67]. Notably, FE-SEM offers six times better spatial resolution than conventional SEM and eliminates the need for coating conductors with insulating materials [67].

The scanning electron microscopy energy dispersive X-ray (SEM-EDX) technique is also utilized to analyze the distribution of elemental composition [64].

3.3.3. Fourier Transform Infrared (FTIR)

Fourier Transform Infrared (FTIR) spectroscopy is employed to analyze the functional groups and variations in chemical behavior on the material surface. This analysis is typically performed within a scan wavelength range of 4000-400 cm^{-1} at a scan rate of 4 s/scan [12,44]. FTIR is also used to examine the surface composition of materials [65].

Raw rice husk samples exhibit intense bands, whereas modified samples display reduced intensity [67]. Table 7 provides a summary of various FTIR peak ranges and their corresponding descriptions.

3.3.3.1. Rice husk functional groups.
The silica surface features two primary functional groups: silanol (Si-O-H) and siloxane (Si-O-Si) [57]. The interaction of silica with other materials is influenced by changes in the silica surface structure, which result from the silica surface reaction with water [70]. Hydroxylation and the formation of a monolayer of adsorbed water on the silica surface alter the surface atomic structure, reducing the adhesion energy [70]. The silanol functional groups on the hydroxylated silica surface are sensitive to small molecules, such as water, under ambient conditions [70].

The surface hydroxyl (OH) groups can be categorized into three types: isolated free (single silanol) hydroxyl groups (SiOH); germinal free (silanediol) Si(OH)$_2$; and vicinal, hydrogen-bonded hydroxyl groups, with the isolated silanol functional group being the most reactive [57]. Siloxane functional groups are formed through the condensation of surface hydroxyl groups due to increasing thermal treatment. While the siloxane functional group on the silica surface is relatively unreactive, the silanol group is the primary site of reactivity on the silica surface [57]. Fig. 10 displays the FT-IR spectrum of a torrefied rice husk.

The FTIR spectrum of pretreated rice husk exhibits a declining trend compared to untreated rice husk, primarily due to the decrease in O/C ratios. Furthermore, the decline in band peaks of pretreated rice husk is attributed to the breakdown of hemicellulose acetyl and uronic ester groups [70].

The Si-OH asymmetric vibration at 3430 cm^{-1} indicates the presence of alcohol. The C=O stretching vibrations at 1730 cm^{-1} are due to the free carbonyl groups, which are abundant in the cellulose and hemicellulose structure of processed rice husk. The C-C vibrations and aromatic ring skeletal vibrations at 1650-1510 cm^{-1} result from the vibrations of aromatic structures from lignin within the rice husk [70].

3.3.4. Higher heating value (HHV)

The Higher Heating Value (HHV) can be determined using a heating value analyzer [44]. Alternatively, the HHV of a material can be calculated using its elemental composition and Dulong's formula [12]. Dulong's formula is as follows[12].

$$HHV = 0.3\,C + 1.428\left[\frac{(H - 0)}{8}\right] + 0.095\,S \tag{1}$$

Heating values of rice husk under various processing conditions is shown in Table 3. The heating values of rice husk samples under torrefied conditions are higher as compared to rice husk processed under higher temperatures. As shown in Table 3, the heating value is higher in sample with less than 30 % oxygen and between 40 and 45 % carbon. Carbon is the most abundant combustible element whereas oxygen is the most abundant incombustible element in rice husk. Higher oxygen content in a sample creates inhibition effect
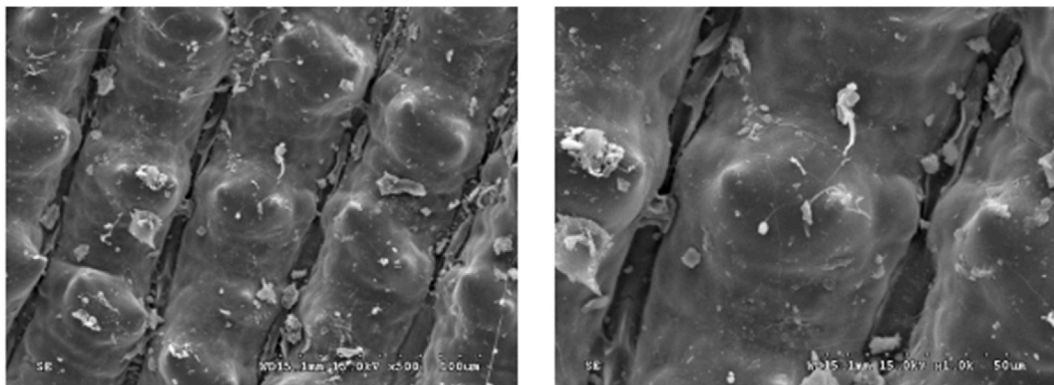

Fig. 9. SEM micrograph of rice husk feedstock as received (Taiwan) (Left x500; Right x1000) [69].

Table 7
Fourier Transform –Infrared peaks description.

Peak average/range (cm^{-1})	Description	Reference
438–476	O-SI-O bending vibration	[6,31,71,72]
466–500	Si-O-Si symmetrical stretching vibration (D4R)	[30,71]
554	Si-O-Si symmetrical stretching vibration (D6R)	[71]
641	Al-O-Si symmetrical stretching vibration	[71]
870	Aromatic ring vibration	[12]
795–972	Si-O-Si symmetrical stretching vibration	[31,50,71,72]
956	Si-OH bending vibrations	[50]
1018	T-O-Si (T: Al or Si) asymmetrical stretching vibration	[71]
1024	0-H vibration	[12]
1045	C-O vibration of hemicellulose and cellulose	[44]
1070–1100	Si-O-Si asymmetric stretching vibrations	[6,50,53,72]
1000–1280	C-O-C stretching vibration	[44,72,73]
1255	C-O vibration of xylan and lignin	[44]
1275	C-O-Si asymmetric stretching vibrations, or CH$_2$ groups	[73]
1310–1490	C – O vibrations	[4]
1376–1393	C- H vibration of hemicellulose, cellulose and lignin	[12,44]
1440–1600	C = C stretching vibration	[72]
1510–1660	C – C vibrations, aromatic rings skeletal vibrations	[4,12,73]
1375–1703	O-H bending vibration	[6,30,44,50]
1735	Ester components of rice husk	[12]
1700–1775	C= O stretching vibrations	[12,72]
2356	Si-H silane hydride vibration	[50]
2300–2450	C ≡ C vibration	[4]
2800–3000	Aliphatic C-H group	[4,12]
3100–3550	O-H stretching vibration	[4,12,44,50,71,73]
3397–3493	Si-OH asymmetric vibration	[30,50]
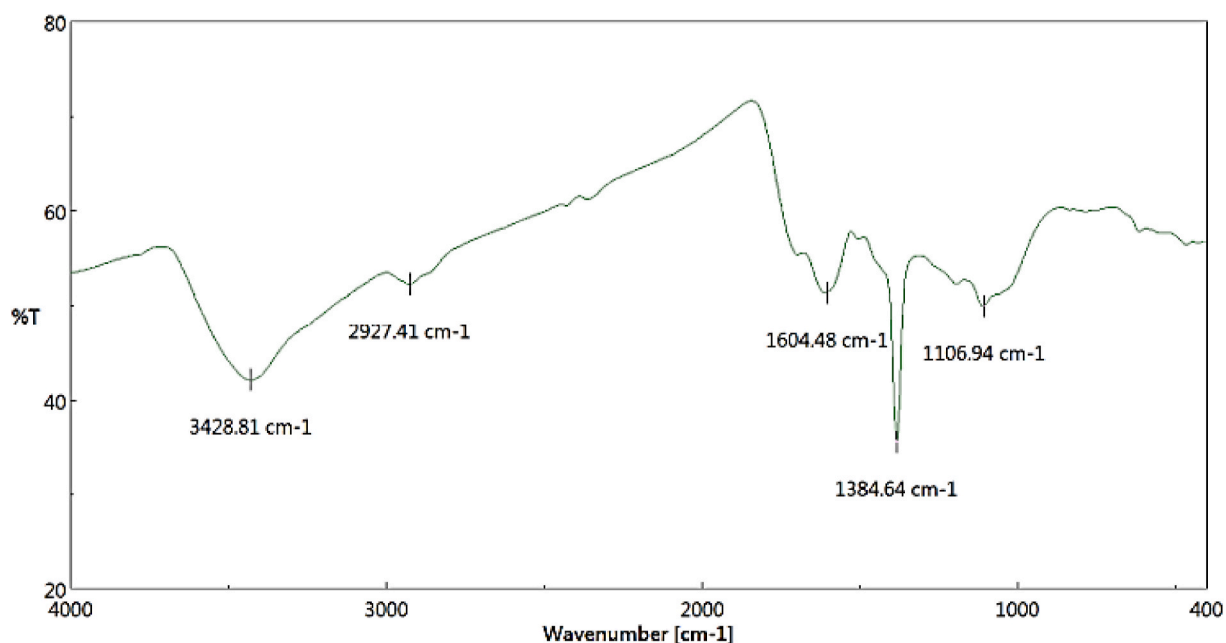
Fig. 10. FTIR spectrum of torrefied rice husk at 280 °C for 30 min [42].

during combustion and thermal decomposition process via incomplete combustion and formation of oxides in the sample [43].

3.3.5. X-ray fluorescence (XRF)

X-ray fluorescence (XRF) is a technique used to analyze the chemical composition and purity of a sample [31,45,74]. Additionally, XRF is employed to determine the oxide composition of materials [40].

Metallic oxide content in rice husk determined via XRF characterization is shown in Table 4. The XRF data in Table 4 indicates the effectiveness of HCl in removing more metallic impurities as compared to other acids such as H$_2$SO$_4$. There is also an increase in silica content (purity) at processing conditions of 600 °C for 2 h to over 99 %.

3.3.6. Brunauer-Emmett-Teller (BET)

Brunauer-Emmett-Teller (BET) analysis is employed to determine the particle size and surface area of a sample [31]. This technique measures the surface area based on nitrogen adsorption by the sample [75]. Additionally, the pore size distribution can be estimated using a BET analyzer [66].

The average pore width is calculated using the formula V_t/S_{BET}, where Vt represents the pore volume calculated at P/Po = 0.99 [76]. Table 6 presents the BET particle size, surface area, and pore volume of pretreated and untreated rice husk calcined at 600 °C.

4. Silicon

Silicon is the most abundant element in the Earth's crust after oxygen [55,78]. Naturally, silicon occurs in its oxide forms, such as silica and silicates, which constitute 25 % of the Earth's crust [55]. Within the silica structure, silicon bonds to four oxygen atoms, with each oxygen atom bonded to two silicon atoms, resulting in a condensed material with the formula SiO_2 [9].

Silicon, analogous to carbon, exhibits oxidation states of 1 and 4 and possesses a cubic, face-centered (FCC), and diamond-type structure. Silicon has a boiling point of 3250 °C and a melting point of 1414 °C, with a density of 2.33 g/cm^3 [55].

High-purity silicon materials, such as Czochralski method-grown monocrystalline silicon crystals, are used in solar photovoltaics and very large-scale integrated circuits (VLSIs) [78]. For solar photovoltaic applications, a suitable high-performance/cost ratio is required [78]. However, for semiconductor applications, such as photovoltaics, extremely high purity is required, with impurities in the ppb range. Consequently, silicon materials like metallurgical-grade silicon, with a purity of 98.5 %–99.5 %, require further purification to achieve over 99.9999 % purity. Several methods are employed for silicon purification, including the Siemens method, which transforms the silicon source material into silicon-chlorine gas, which is then distilled and reduced to produce high-purity silicon [55].
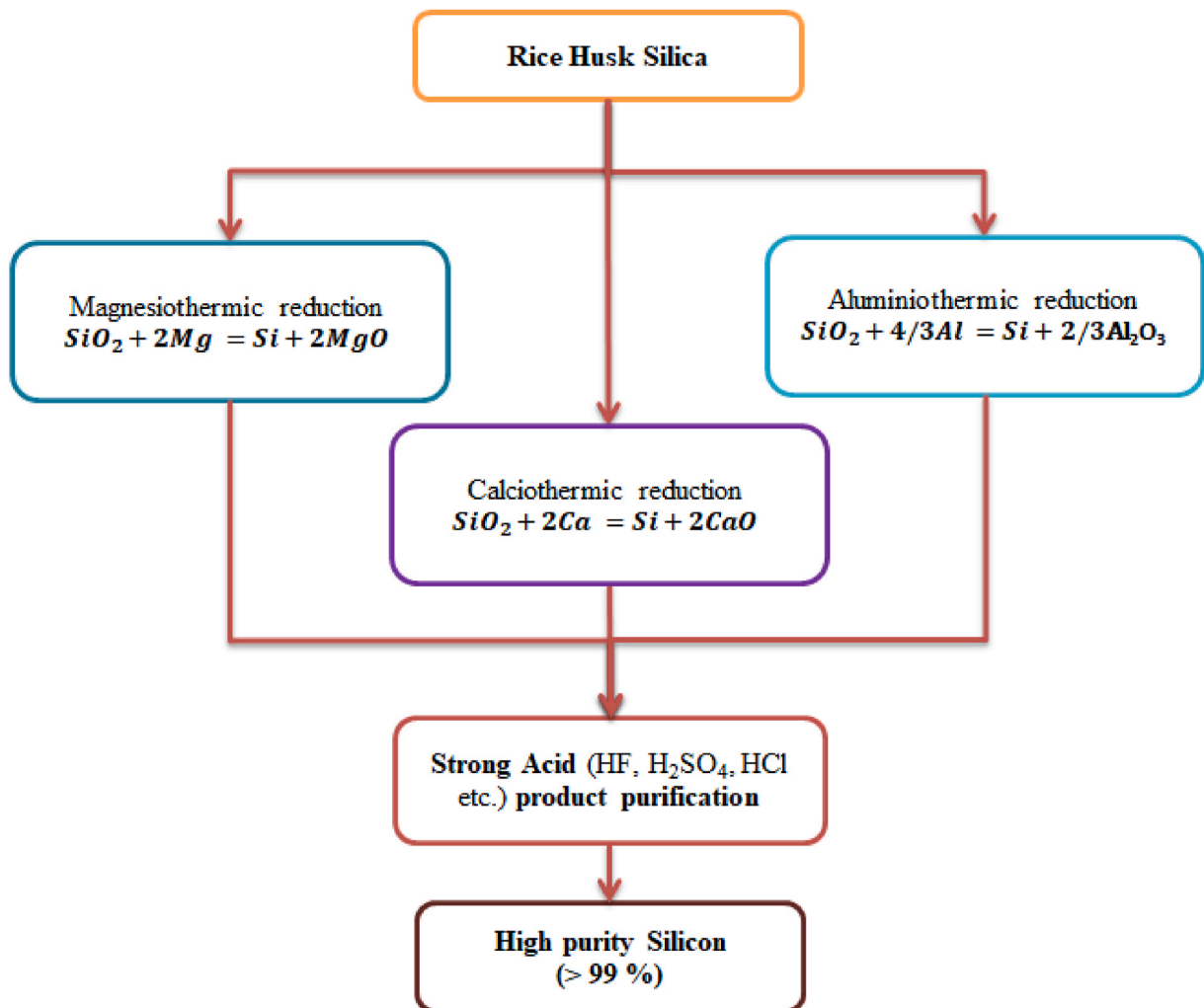

Fig. 11. Schematic of silicon synthesis rom rice husk silica.

Directional solidification (DS) is another method that has gained attention over the past decade for growing customized silicon crystals. This method utilizes less pure materials compared to the Czochralski method. Quartz, produced by slip casting, is used as the crucible, which is coated with silicon nitride to prevent sticking with the solidified silicon. However, impurities such as phosphorus, boron, and aluminum, as well as impurities from graphite used in the hot zone, are introduced during this process. Structural defects, including grain boundaries (GB) and dislocations, are also introduced, acting as recombination centers for light-generated holes and electrons, which affects solar cell performance [78].

Conventional silicon synthesis methods are energy-intensive, resulting in high production costs. Therefore, there is a need to reduce production costs through the use of low-cost raw materials, improved synthesis processes, and comparable silicon purity [11].

4.1. Silicon synthesis from rice husk

Silicon extracted from rice husk ash (RHA) silica reduction provides a simple and cost-effective means of synthesizing silicon. The reduction of RHA silica to silicon involves boiling water wash/acid milling purification processes and carbothermal thermic reduction. However, carbothermal reduction distorts the morphology of the silicon due to the liquefaction of the silicon in the process [14].

Conventional carbothermal reduction of silica to silicon is highly energy-intensive [2,3,21], expensive [2,3], and associated with high pressure and temperature [2,79], eco-hazardous [21], and strong acidity [2]. Therefore, it is essential to decarbonize the silicon manufacturing process [21] using alternative silicon synthesis methods that are less energy-intensive and costly, with high volume and lower carbon emissions [3].

Among the methods for silicon synthesis is reduction using metals such as Mg, Ca, Ti, and Al at relatively lower temperatures [11]. The metallothermic reduction methods include aluminothermic (using aluminum), magnesiothermic (using magnesium metal), and calciothermic (using calcium metal) [3,14]. Fig. 11 shows a schematic of the synthesis of silicon via the reduction of silica using Mg, Ca, and Al.

Aluminothermic reduction of rice husk silica is carried out at 650 °C for 3 h, yielding silicon with 46.72 % purity [35]. Rice husk silica (rice husk white ash) is mixed with a reducing metal such as Ca or Mg, typically with a 5 % excess stoichiometry. The mixture is then heated at temperatures between 700 °C and 800 °C to produce silicon. Mixtures of various acids (HF, H_2SO_4, HCl, etc.) are used to remove remaining metallic impurities and unreacted reducing metals, yielding highly pure silicon [3].

Magnesiothermic reduction of silica/carbon composites to form silicon carbide and silicon/carbon materials is useful in non-metal oxide ceramics and lithium-ion batteries (LIBs), respectively [14]. Magnesiothermal reduction of silica at temperatures between 500 °C and 950 °C yields porous structured silicon [35]. Magnesiothermal reduction has gained attention due to the relatively low temperature of 650 °C used in the process [14,20], compared to the over 2000 °C used in carbothermic reduction [14].

At temperatures between 600 °C and 650 °C, the melting and directional solidification of silicon occur with boron as an active impurity [20]. However, magnesiothermal reduction products, such as Mg_2Si (which is unstable and reacts readily with air), reduce the overall silicon yield and affect the silicon product morphology [35].

Several factors influence the silicon yield from magnesiothermal reduction, including reaction temperature (500–900 °C), ramp heating rate (1–4 °C/min), molar ratio of magnesium to silica (1.5–3), and reaction time (0.5–12 h) [35]. At lower temperatures, silicon is intertwined with the magnesia phase, with particle sizes ranging from 2 to 50 nm. However, increasing the temperature causes magnesia crystallites to aggregate into macropores, approximately 200 nm in size [35].

In the magnesiothermic reduction process, magnesium metal is placed adjacent to the silica material in a furnace at 650–800 °C. During the process, magnesium vaporizes. However, zonal variations occur, with unreacted silica present farther from the magnesium, silicon in the middle, and Mg_2Si near the magnesium. The addition of NaCl prevents the temperature from exceeding 801 °C, thereby preventing the melting of silicon and distortion of the silica morphology. NaCl serves as a heat scavenger. A mixture of various acids, such as HF, H_2SO_4, and HCl, is used to remove MgO, unreacted Mg, and Mg_2Si, yielding highly pure silicon (99.999 %) [35]. The silicon synthesized via magnesiothermic reduction exhibits a three-dimensionally structured Si replica [14].

$$SiO_2 + 2Mg = Si + 2MgO + SiO_{2(unreacted)}$$ [3]

Olawale et al. [51] produced microcrystalline silicon from rice husk silica through a multi-step process. Initially, the silica was chemically treated with oxalic acid and then carbonized at 700 °C for 3 h, with a heating rate of 10 °C/min. Subsequently, the silica underwent magnesiothermal reduction via pyrolysis at 650 °C for 3 h, using 99 % pure magnesium. Raman spectroscopy and SEM analysis revealed that the produced silicon was microcrystalline and porous, respectively.

4.2. Silicon characterization

Several tests have been conducted on rice husk silicon, including electrical conductivity. Electrical conductivity refers to a material's ability to conduct electric current. Materials are categorized into insulators, semiconductors, and conductors based on their electrical conductivity, which ranges from 10^{-9} S/cm to 10^3 S/cm for insulators, 10^{-9} S/cm to 10^3 S/cm for semiconductors, and above 10^3 S/cm for conductors [35].

The electrical conductivity of rice husk ash has been measured to be 0.205×10^{-7} S/cm to 1.48×10^{-7} S/cm, which is relatively low compared to quartz sand, which has an electrical conductivity of 1.2×10^{-5} S/cm [35].

The bandgap energy, which is the difference between the conduction band and the valence band, determines the transition energy required to convert a valence band electron into a conduction band electron. The bandgap energy ranges from 4 eV for insulators, 0–4

eV for semiconductors, and 0.5 eV for conductors [35].

An LCR meter is used to measure the electrical conductivity of materials by measuring inductance (L), resistance (R), and capacitance (C). The conductance value (G) determined by the LCR meter is obtained using the standard resistance value (R) [35].

5. Silica/silicon based materials

Rice husk serves as a precursor material for the synthesis of various valuable materials, including silicon nitride, silica glass, silicon carbide, zeolites, magnesium silicate, pure silicon, and silicon tetrachloride [50].

5.1. Silica as a ceramic material

Silica, due to its low thermal conductivity, is utilized in refractories, which serve as secondary linings in kilns or furnaces. Silica is regarded as the backbone of the ceramic industry and is a crucial ingredient. Conventional sources of silica in the ceramic industry include quartz, granite, silica sand, gravels, and quartzite. However, the use of these raw materials poses a threat to their exploitation and depletion [10].

The reactivity of amorphous silica increases its relevance in the ceramic industry. Although fused silica, which is amorphous, is used in the ceramic industry, it is expensive. Rice husk, an agricultural waste, provides a cost-effective solution to this challenge [10].

5.2. Silicon carbide

Silicon Carbide (also known as carborundum) exhibits exceptional properties, including a high decomposition temperature (2830 °C), favorable oxidation resistance, high-temperature stability, and favorable neutronic and irradiation properties [80]. Notably, Silicon Carbide decomposes at 2545 °C but does not melt [55]. These characteristics make it an ideal material for various applications, including next-generation structural composites, electronics heating elements, thermal management, brakes, and abrasive liners [80].

Silicon Carbide, synthesized via carbothermal reduction of silica with carbon, is a promising ceramic material used in various applications, such as composite reinforcement, electronic devices, optic devices, and catalyst support [2]. Fig. 12 presents the SEM micrograph and XRD diffractograph of Silicon Carbide.

Environmental barrier coatings (EBCs) are synthesized from a Si bond coat and a volatilization barrier, such as mullite. EBCs are used to shield SiC/SiC ceramic matrix composites (CMCs) from surface recession in the hot sections of gas turbine engines [81].

Conventional silicon carbide (SiC) is synthesized via the Acheson method, which involves smelting a mixture of coal (carbon source) and quartz at 2400 °C [10]. In the conventional SiC synthesis approach, petroleum coke and quartz are used as the carbon and silica sources, respectively, in a carbothermal reduction process using an electrical resistance furnace [2].

The silicon carbide formation temperature can be decreased through the addition of rice husk [10]. The use of rice husk in SiC synthesis involves coking (to eliminate volatiles) between 400 and 800 °C, followed by a high-temperature reaction above 1300 °C to form SiC. The carbothermal reduction can occur at 1500 °C for 15 min or 1300 °C for 60 min [2].

The carbothermal reduction process in SiC synthesis involves four stages.

i. Cristobalite formation from the crystallization of silica (temperature between 1000 and 1200 °C)
ii Amorphous carbon graphitization (temperature >1300 °C)
iii. SiC whiskers formation (temperatures between 1200 and 1400 °C)
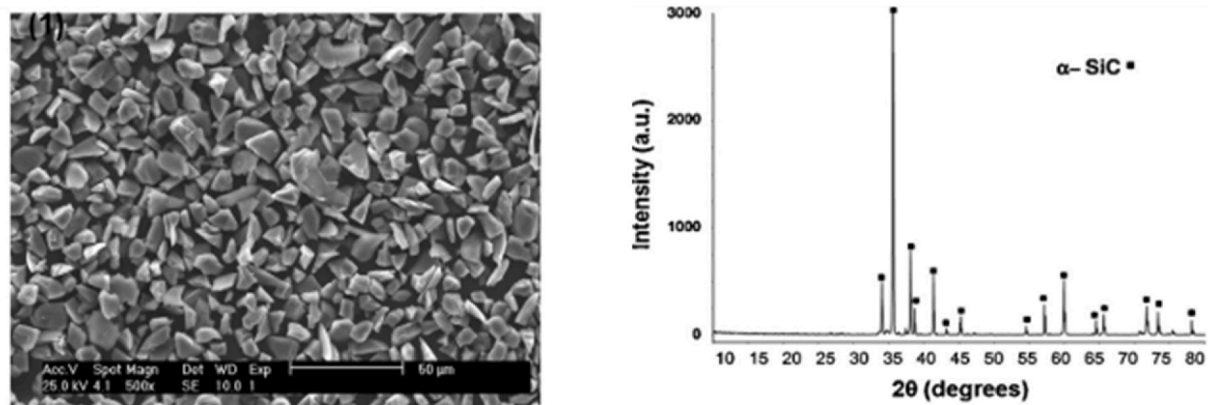iv. SiC particulates (alpha and beta) formation (temperature higher than 1400 °C)

Fig. 12. SEM micrograph and XRD diffractograph of Silicon Carbide (Left: SEM micrograph of SiC; Right: XRD pattern of SiC) [68].

The formation of CO is desirable for silicon carbide whiskers formation. Controlling SiO vapor release due to sustained contact between silica and carbon increases silicon carbide whiskers formation. Additionally, the absorbed SiO in carbon pores leads to the formation of silicon carbide particles. SiC whiskers formation from pyrolyzed treated rice husk precursor is higher than pyrolyzed untreated rice husk precursor. However, the SiC whisker formation from acid-treated rice husk is lower than untreated rice husk [3].

Other SiC synthesis methods involve infiltrating carbon porous preforms or SiC with Si to react with the carbon. In this process, pyrolyzed rice husk containing SiC whiskers, carbon, and particles is infiltrated with molten Si to synthesize SiC ceramic composites [11].

5.3. Silica nanowires

One-dimensional (1D) nanostructured materials, including nanowires, nanorods, nanoribbons, and nanotubes, have garnered significant attention due to their unique properties. Nanowires are particularly useful for analyzing the dependence of thermal, electrical, and mechanical transport properties on size confinement and dimensionality. Furthermore, nanowires play a crucial role in nano-optoelectronic devices and nanoelectronics functionality and integration [50].

Various methods have been employed for nanowire synthesis, including vapor-liquid-solid (VLS), sol-gel, electro deposition, and chemical vapor deposition (CVD). However, the hydrothermal method offers a highly efficient and cost-effective approach for the anisotropic growth of 1D nanostructures [50].

Bathla et al. [50] successfully synthesized silica nanowires using a Fe_2O_3-assisted hydrothermal process with Edamine as the solvent. The resulting nanowires exhibited diameters ranging from 15 to 35 nm and lengths of approximately 0.5 μm. Fourier-transform infrared spectroscopy (FTIR) analysis revealed the presence of siloxane, silanol, and H-bonded hydroxyl functional groups, characterized by symmetric and asymmetric stretching bonds.

5.4. Silicon nitride

Silicon Nitride is a non-oxide ceramic material that exhibits exceptional properties, including high thermal shock resistance, high strength at elevated temperatures, high creep resistance, a low thermal expansion coefficient, and high corrosion resistance. Due to these characteristics, Silicon Nitride is particularly suitable for high-temperature structural ceramic materials [10].

Carbothermal-nitridation, a method requiring high-purity carbon and silica, is commonly employed for Silicon Nitride synthesis. Rice husk, an agricultural waste containing both carbon and silica, presents a promising alternative for Silicon Nitride synthesis. The synthesis process involves pyrolyzing rice husk, followed by thermal treatment at high temperatures (1400–1470 °C) in a nitrogen and hydrogen gas environment [10].

5.5. Silica aerogel

Rice husk silica is utilized in the synthesis of silica aerogel, an ultra-light material characterized by its low bulk density (0.03–0.5 g/cm³), high specific surface area (500–1500 m^2/g), low dielectric constant, low thermal conductivity, and high porosity (80–99 %) [10].

Silica aerogel finds applications as a catalyst support, pollutant adsorbent, drug carrier, membrane, and in microelectronics. The synthesis of silica aerogel from rice husk silica involves several steps. Initially, rice husk silica is extracted as sodium silicate using sodium hydroxide. Subsequently, sodium ions are removed through a neutralizing or cation exchange resin method using an acid to form silica hydrosol. Tetraethyl orthosilicate (TEOS) is then added to form a gel, which is washed with ethanol or water and dried to obtain silica aerogel [2].

Rice husk-derived carbon-silica (C/SiO_2) composites have been explored as anode materials in lithium-ion batteries [10]. The sol-gel polymerization of silicon alkoxides is a common method for synthesizing silica aerogel. Rice husk ash (RHA) has been employed as a silicon source in silica aerogel synthesis through a sol-gel method. This involves the use of an acid to form silica hydrosol, followed by the addition of a small amount of TEOS to form a gel. The gel is then aged, hydrolyzed, and undergoes condensation reactions to form siloxane bonds [2].

6. Other application of rice husk derived products

6.1. Zeolites

Zeolites are versatile materials used as adsorbents for pollutant removal, petroleum upgrading, and catalyst synthesis [2]. At high temperatures, activated carbon as a CO_2 adsorbent exhibits poor thermal stability [71]. In contrast, zeolites possess superior ion exchange capacity, thermal stability, and chemical stability [71].

Zeolites are typically synthesized from the reaction of sodium silicate and aluminate. However, alternative aluminosilicate sources, such as rice husk ash (RHA), have also been employed [2]. RHA has been used as a precursor material in the synthesis of Zeolite NaY [1].

Zeolites are microporous materials characterized by their regular arrangement of pores, cages, and channels in molecular dimensions [82]. They are hydrated, cross-linked, open framework structures of crystalline aluminosilicates, comprising TO_4 (T: Si/Al) units with corner-sharing AlO_4 and SiO_4 tetrahedral [1,2,83].

Zeolite Y, a member of the faujasite family, exhibits a high degree of versatility as a molecular sieve, featuring a 3D pore structure

[1]. The faujasite (FAU) family of zeolites is characterized by pores running perpendicular to each other in the x, y, and z planes, forming a 3D pore structure. The pore diameter is approximately 7.4 Å, with a 12-member oxygen ring forming a large cavity with a diameter of 12 Å [83]. Other members of the faujasite family include NaX and NaY [2].

Zeolite Y is a versatile molecular sieve with a 3D pore structure, exhibiting solid acidity and finding applications in ion exchange, adsorption, and catalyst synthesis [2]. Zeolite Y is synthesized with high aluminum content and is employed as a catalyst, adsorbent, and ion exchanger [1]. Zeolite Y thermally decomposes at 793 °C, with a void volume fraction of 0.48 and a Si/Al ratio of 2.43 [83].

Mohamed et al. [1] synthesized Zeolite Y using rice husk silica due to its strong reactivity with NaOH to form sodium silicate. The optimal crystallization conditions for zeolite Y synthesis were found to be 24 h at 110 °C, yielding a surface area of 716.6 m^2/g. The synthesized zeolite Y exhibited a uniform and homogeneous particle size distribution.

In another study, Rahman et al. [83] used 10 % sulfuric acid-pretreated, highly amorphous RHA silica with 95.8 % purity as a precursor in the synthesis of zeolite Y. The results showed that zeolite Y synthesized with seeding yielded highly pure zeolite Y with maximum crystallinity, whereas synthesis without seeding yielded zeolite P and zeolite Y.

Madhu et al. [71] synthesized zeolite for CO_2 adsorption from rice husk silica source via a hydrothermal method using an organic template. The synthesized zeolites RA and RX exhibited BET surface areas of 106.25 m^2/g and 512.79 m^2/g, respectively, with CO_2 adsorption capacities of 2.22 and 2.45 mmol/g, respectively, at 297.15 K temperature.

6.2. Biochar, fertilizers for soil remediation and improvement

Biochar is produced through the incomplete combustion (thermochemical conversion) of biomass, such as rice husk, in an oxygen-deficient environment at temperatures above 250 °C. Thermochemical conversion processes that yield biochar include pyrolysis, dry combustion, and gasification [13].

The porous structure of biochar enhances soil health by adjusting soil pH, reducing greenhouse gas emissions, retaining water and fertilizers, improving soil cation exchange capacity (CEC), and increasing carbon stability in soil. Additionally, biochar serves as a long-term carbon sink, as evidenced by millennial-scale stability studies. Biochar containing nitrogen, phosphorus, and potassium is also used as a source of soil nutrients. Furthermore, biochar can remove pollutants and heavy metals during the soil amendment process [14].

6.3. Catalyst and catalyst support

Catalysts are a significant expense in the conversion of biomass into valuable products [14]. However, rice husk ash (RHA) can be utilized to synthesize nano-sized solid acid catalysts through acid activation. These catalysts are essential for the transesterification of free fatty acids (FFA) with methanol to produce biodiesel [13].

The use of silica-rich RHA as a modifying catalyst in the synthesis of value-added products from biomass reduces costs and makes it an economically viable venture. RHA can be modified as a solid acid catalyst for biodiesel production, which involves low-temperature esterification of free fatty acids (FFA). Additionally, RHA catalysts are effective in converting tars in the pyrolysis process for syngas (vapor) upgrade in power generation [14].

Silica is also used as a support for transition metals, such as titanium and chromium, to produce heterogeneous catalysts. The sol-gel technique, which involves silica precipitation and transition metal incorporation into the silica framework, provides a high degree of control over the resulting catalyst properties. Transition metals commonly used include chromium, molybdenum, tungsten, iron, and cobalt [57].

6.4. Detergent additive

In a study by Deng et al. [84], rice husk silicon was utilized as a precursor material in the synthesis of δ-$Na_2Si_2O_5$, a potential builder in detergents. δ-$Na_2Si_2O_5$, a polymeric layered crystal structured compound, exhibits excellent washing properties, including pH buffering capacity, binding Ca^{2+} and Mg^{2+}, high solubility, and a 4 Å zeolite structure, making it an effective builder in detergents. δ-$Na_2Si_2O_5$ was synthesized from rice husk ash (RHA) through sintering at 720 °C for 120 min, with a broad exothermic peak observed at 715 °C. The synthesized δ-$Na_2Si_2O_5$ sample demonstrated excellent Mg^{2+} and Ca^{2+} binding capacities, with values of 435 mg/g and 396 mg/g, respectively [84].

6.5. Cement/concrete application

The global demand for concrete is projected to rise to 18 billion tonnes by 2050, driven by population growth, urbanization, and infrastructure development [85]. Cements account for 20–40 % of the total volume of cementitious mortar or concrete [85]. However, cement production is energy-intensive, relies on non-renewable resources like limestone, and generates significant CO_2 emissions, contributing to approximately 7 % of global carbon emissions [85].

The cement manufacturing industry faces challenges such as excessive utilization of non-renewable resources and increased carbon emissions. The use of agro-waste materials like rice husk can help address these challenges. However, the increased use of agro-waste in biomass-based energy plants has led to a rise in agro-waste ash disposal [40].

Rice husk ash (RHA) is used as a pozzolan in cement production due to its pozzolanic behavior, which is attributed to the amorphous silica present in RHA [40]. Pozzolans are finely divided aluminous and siliceous materials that react chemically with

calcium hydroxide in the presence of moisture to form cementitious compounds at ordinary temperatures [38].

Rice husk silica with a purity of more than 97 wt% is desirable as a pozzolan in concrete [13]. The pozzolanic properties of bio-waste ash are influenced by production processes [22]. To achieve desirable pozzolanic activity of RHA, factors such as incineration temperature, time, processing, and grinding of RHA must be controlled [16].

Pozzolans react with free lime to form insoluble compounds, making the cement more resistant to environmental degradation [38]. RHA has high pozzolanic activity, which depends on factors such as particle fineness, available alkaline media, amorphous silica content, and mix proportions [16].

The high silica content in RHA gives it pozzolanic properties, making it a valuable additive in cement production [22]. Biogenic silica from rice husk has a high surface area and is highly reactive [21]. The reactivity of RHA silica depends on temperature and heating duration [52].

When RHA reacts with calcium hydroxide, it forms C-S-H gel, which is porous and has a large surface area [38]. The formed C-S-H gel enriches the concrete microstructure, enhancing its sulfate resistance [40]. Additionally, the plasticity of cement is increased, and the heat of hydration is reduced [38].

The ultrafine nature of rice husk ash (RHA) as a pozzolan makes it a suitable micro-void filler, yielding high concrete strength [38]. Mechanical grinding of RHA decreases particle sizes, increases fineness, and enhances specific surface area, ultimately increasing pozzolanic activity [16]. Prolonged grinding of RHA leads to the breakdown of its porous cellular structure, resulting in reduced water requirements for concrete with the same workability [40].

Controlling RHA fineness affects water demand in concrete. Increasing RHA fineness enhances its reactivity, which is highly attributed to its amorphous silica content and porous nature, resulting in a high surface area. Adding 3 % RHA by mass to cement does not adversely affect water demand in concrete. However, adding 30 % RHA by mass to cement substantially reduces water demand, chloride permeation, and chloride diffusion in concrete [52].

Amorphous silica synthesized from hydrochloric acid pretreatment of rice husk exhibits enhanced and stable pozzolanic activity [86]. The high reactivity of amorphous RHA influences increased consumption of calcium hydroxide during OPC hydration, accelerating strength gain in RHA-OPC [52]. Amorphous silica has a solubility range of 70–150 mg/kg, while crystalline silica has a solubility of 10 mg/kg at 25 °C [13].

Amorphous silica with 35 μm particle sizes is used in high-performance concrete, which has low operability, high strength, and is useful in nuclear power plants, marine, and bridge structures construction [13]. Adding up to 30 % RHA silica decreases permeability, improves corrosion resistance and strength, and reduces chloride penetration [3]. Pozzolanic admixtures generally enhance concrete strength and durability [52].

Rice husk ash impurities, such as aluminum, improve mechanical strength through the formation of aluminosilicates. However, the presence of alkali oxides in RHA has a negative impact on hydration rate and setting, with oxides of Fe, Al, and S having the least effect on hydration. Complete combustion of rice husk yields 20–25 % RHA, containing approximately 90 % silica, with fine particles, high reactivity due to its amorphous silica nature, and suitable cement-concrete compatibility, making it a desirable pozzolana material [16].

Adding RHA to cement concrete improves durability and mechanical properties against adverse environmental conditions. A 10–25 % replacement of ordinary Portland cement (OPC) with RHA is recommended [16]. Incomplete combustion of rice husk below 500 °C results in unburnt carbon, which reduces its pozzolanic activity. Further thermal treatment of incomplete combustion of rice husk reduces unburnt carbon, increasing silica content. RHA synthesized at 500 °C for 120 min achieved maximum desirable fineness, maximum density, maximum amorphous silica content, with enhanced pozzolanic effect and least production energy [52].

RHA density can be used as a measure of its amorphous state, as higher density indicates higher amorphous content. The density of RHA typically ranges between 1.1 and 1.9 kN/m^2 [52]. One measure of pozzolanic activity is the decrease in electrical conductivity of a saturated Ca(OH)$_2$ solution with RHA [16]. The pozzolanic activity of RHA is estimated by pore size distribution of the mortar, hydration heat, and heat evolution of cement, and Ca(OH)$_2$ content in the mortar after reaction. The activeness of RHA is directly proportional to the change in saturated Ca(OH)$_2$ conductivity [16].

The impurities content of rice husk, an agro-waste, can be reduced through acid leaching of the husk [86].

The Strength Activity Index (SAI) which is the ASTM measure o the pozzolanic behaviour of supplementary cementitious material is however low in RHA pozzolan mortar. A reported SAI of 58 % of RHA pozzolan mortar is below the ASTM standard of 75 %. This is due to the presence of carbon which can be corrected through appropriate treatment of the RHA. The optimum calcination temperature of rice husk for pozzolana material is between 600 and 700 °C with an optimum rice husk silica replacement level of 10–20 %. Higher calcination duration leads to specific surface area increase of RHA making it more conducive as a pozzolan due to reduction of unburnt carbon [40].

In Muthukrishnan et al. [85] research, thermally treated industrial rice husk ash (rice husk ash from industrial boilers for energy generation) was used as an admixture in cement production. Also rice husk biochar and industrial rice husk ash were mixed, and used in cement production. The thermally treated industrial rice husk ash improved the mortar strength by 20 % and 34 % after early stage of 7 days and mature age of 120 days respectively. The mixture of rice husk biochar and industrial rice husk ash improved the water retention and compressive strength by 23 % and 17 % respectively.

The Strength Activity Index (SAI), an ASTM measure of the pozzolanic behavior of supplementary cementitious materials, is relatively low in RHA pozzolan mortar. A reported SAI of 58 % for RHA pozzolan mortar falls below the ASTM standard of 75 %. This is attributed to the presence of carbon, which can be corrected through appropriate treatment of the RHA [40].

The optimal calcination temperature for rice husk to produce pozzolana material is between 600 and 700 °C, with an optimal rice husk silica replacement level of 10–20 %. Prolonged calcination duration increases the specific surface area of RHA, making it more

conducive as a pozzolan due to the reduction of unburnt carbon [40].

In a study by Muthukrishnan et al. [85], thermally treated industrial rice husk ash (RHA from industrial boilers for energy generation) was used as an admixture in cement production. Additionally, a mixture of rice husk biochar and industrial RHA was used in cement production. The thermally treated industrial RHA improved mortar strength by 20 % and 34 % after 7 days and 120 days, respectively. The mixture of rice husk biochar and industrial RHA improved water retention and compressive strength by 23 % and 17 %, respectively.

6.6. Medicine and drug delivery

The increasing demand for nanomaterials in fields like biomedicine has driven the evolution of green technology and nano-medicine. In medical treatment, drug molecules are incorporated into silica matrices via microemulsion or the Stober method, serving as drug carriers due to their quick, targeted, and controllable release rates and delivery [87]. Nanomaterials are used in tissue engineering and therapy, leveraging their high surface area and volume ratio advantages as nanocarriers (for drugs, proteins, etc.) [88].

Silica nanomaterials are nontoxic, biocompatible, and do not absorb light, making them suitable for biomedical research [13]. Silica nanoparticles, including Cornell dots (Cdots), are ultrasmall fluorescent core-shell silica nanoparticles used as nanocarriers in drug delivery [88]. Amorphous silica, being non-toxic with easily modified surfaces, is more desirable in synthesizing drug carriers [87].

Rice husk nanosilica materials, hybridized with various functional molecules, are used in drug delivery, catalysis, cancer therapy, biosensing, and bioimaging. The high porosity of amorphous silica provides a suitable three-dimensional space matrix for doping functional groups/molecules, including drug molecules, fluorophores, and photosensitizers [87].

Amorphous nanosilica bioactive materials from rice husk exhibit a bone-like hydroxyapatite (HyA) layer on their surface, bonding to living bone tissues through the apatite layer during implants. Rice husk-based nanosilica HyA is biodegradable and highly bioactive compared to calcium phosphate biomaterials. The optimal synthesis route for nanosilica HyA using rice husk ash as a silica precursor involves a sintering temperature of 950–1000 °C and sol-gel synthesis [2].

Silica has also been used in gene delivery for more efficient DNA delivery vectors in research and clinical trials. The high density of surface silanol groups (Si-OH) on amorphous silica enhances the formation of hydroxyapatite (HAp) and bone in bioglass and glass ceramic systems [30]. Rice husk ash delivers orthosilicic acid ($Si(OH)_4$) in high solubility, making it useful in wound dressing and healing, particularly for non-healing diabetic wounds and bacterial-infested wounds due to its antimicrobial properties [89].

Ali & Drea [89] synthesized rice husk silica by ashing in a muffle furnace at 700 °C for 3 h, then treated with NaOH at 100 °C for 4 h to produce sodium silicate, then finally treated with 5 N sulfuric acid in a reflux method to yield high purity silica. The FTIR showed symmetric and asymmetric siloxane vibrations at 808.20 cm^{-1} and 1072.46 cm^{-1}. The synthesized silica content was 91 % with traces of minerals. The synthesized nanosilica demonstrated antibacterial efficacy with a concentration of 62.5 μ g/ml against gram-negative *Escherichia coli* bacteria. The synthesized silica was also useful in wound dressing and antibiotic.

In a study conducted by Unglaube et al. [26], a nanosized silver-containing silica/carbon composite with antimicrobial properties was synthesized. This was achieved by mixing rice husk precursor with varying amounts of $AgNO_3$ and ethanol at 600 °C, with a heating rate of 10 °C/min. Silver ions (Ag) were directly applied to the lignocellulose framework of rice husk.

The resulting material underwent carbothermal reduction to synthesize silica/carbon composites. The silica/carbon composite was then doped with silver nanoparticles (AgNps) as active agents. XRD analysis revealed broad peaks between 15° and 30°, indicating an amorphous silica material. Cubic reflexes peaks were also observed at 38.1°, 44.3°, 64.5°, and 77.5° [26].

The material exhibited a BET surface area of 260.7 m^2/g, with a pore volume of 0.05 cm^3/g for pores between 2 nm and 100 nm. Microbial analysis tests demonstrated the growth inhibition of gram-positive bacteria (*Enterococcus faecium, Staphylococcus aureus*) and gram-negative bacteria (*Pseudomonas aeruginosa, Escherichia coli*). Notably, no detectable Ag amounts were detected after the microbial analysis, indicating that the growth inhibition was related to the presence of Ag [26].

7. Conclusions

This review highlighted the formation of silica in rice plant, the thermochemical extraction of silica from rice husk and the reduction of silica into silicon. The various characterization techniques were also discussed. The synthesis of various advanced materials such as silicon carbide, activate carbon, zeolites were also outline and their used in various process discussed. Among the highlight are.

- Rice husk ash is a significant and renewable resource in silica synthesis.
- Rice husk ash is essential in various applications such as cement manufacturing as pozzolan, catalyst support and drug carriers in medicine delivery.
- Chemical pretreatment of rice husk is very effective as compared to water soaking in removing alkali impurities in rice husk.
- The pretreatment step and silica extraction approach affect the morphology and purity of the extracted rice husk silica.
- Factors such as carbonation temperature and carbonization duration/residence time affects the structure of the silica – whether amorphous or crystalline.
- Alkali impurities such as potassium influence the trapping of carbon in silica surface melt leading to incomplete combustion which affects the purity and colour of the rice husk ash.

- In the synthesis of activate carbon, rice husk ash is leached out using chemicals such as HF to improve the rice husk carbon component.
- The use of reducing metals such as Mg, Ca an Al in silica reduction to Si requires lower temperature and is less energy intensive as compared to the conventional carbothermal Si synthesis method.

CRediT authorship contribution statement

Ibrahim Hamidu: Writing – review & editing, Writing – original draft. **Benjamin Afotey:** Supervision. **Bright Kwakye-Awuah:** Supervision. **Daniel Adjah Anang:** Supervision.

Data availability statement

Data will be made available on request. For requesting data, please write to the corresponding author.

Research funding

Declaration of competing interest

The authors declare that they have no known competing financial interests or personal relationships that could have appeared to influence the work reported in this paper.

References

[1] R.M. Mohamed, I.A.M. Khalid, M.A. Barakat, Rice husk ash as a renewable source for the production of zeolite NaY and its characterization, Arab. J. Chem. (2013), https://doi.org/10.1016/j.arabjc.2012.12.013.

[2] Y. Shen, P. Zhao, Q. Shao, Porous silica and carbon derived materials from rice husk pyrolysis char, Microporous Mesoporous Mater. 188 (2014) 46–76, https://doi.org/10.1016/j.micromeso.2014.01.005.

[3] N. Soltani, A. Bahrami, M.I. Pech-Canul, L.A. González, Review on the physicochemical treatments of rice husk for production of advanced materials, Chem. Eng. J. (2014), https://doi.org/10.1016/j.cej.2014.11.056.

[4] Y.E. Sknar, T. V Hrydnieva, I. V Sknar, P. V Riabik, O. V Demchyshyna, Characteristics of silicon dioxide produced from rice husk, J. Chem. Technol. 30 (1) (2022) 103–109, https://doi.org/10.15421/jchemtech.v30i1.251588.

[5] L.N.A. Tuan, L.T.K. Dung, L.D.T. Ha, N.Q. Hien, V.D. Phu, B.D. Du, View of Preparation and characterization of nanosilica from rice husk ash by chemical treatment combined with calcination.pdf, Vietnam J. Chem. 55 (4) (2017) 455–459, https://doi.org/10.15625/2525-2321.2017-00490.

[6] U. Zulfiqar, T. Subhani, S.W. Husain, Synthesis of silica nanoparticles from sodium silicate under alkaline conditions, J. Sol. Gel Sci. Technol. (2016) 1–6, https://doi.org/10.1007/s10971-015-3950-7.

[7] T. Liou, C. Yang, Synthesis and surface characteristics of nanosilica produced from alkali-extracted rice husk ash, Mater. Sci. Eng. B 176 (7) (2011) 521–529, https://doi.org/10.1016/j.mseb.2011.01.007.

[8] Y.E. Sknar, T. V Hrydnieva, A.O. Liashenko, P. V Riabik, I. V Sknar, Y.A. Hrydniev, Study of the kinetics of thermal decomposition of the rice husks purified from cellulose, J. Chem. Technol. 29 (1) (2021) 128–136, https://doi.org/10.15421/082112.

[9] B.S. Todkar, O.A. Deorukhkar, S.M. Deshmukh, Extraction of silica from rice husk, Int. J. Eng. Res. Dev. 12 (3) (2016) 69–74.

[10] S.K.S. Hossain, L. Mathur, P.K. Roy, Rice husk/rice husk ash as an alternative source of silica in ceramics : a review, J. Asian Ceram. Soc. 6 (4) (2018) 299–313, https://doi.org/10.1080/21870764.2018.1539210.

[11] N. Soltani, A. Bahrami, M.I. Pech-Canul, L.A. González, Review on the physicochemical treatments of rice husk for production of advanced materials, Chem. Eng. J. 264 (2015) 899–935, https://doi.org/10.1016/j.cej.2014.11.056.

[12] Z. Xu, Y. Tan, X. Ma, S. Wu, B. Zhang, The influence of NaCl during hydrothermal carbonization for rice husk on hydrochar physicochemical properties, Energy 266 (April 2022) (2023) 126463, https://doi.org/10.1016/j.energy.2022.126463.

[13] R. Pode, Potential applications of rice husk ash waste from rice husk biomass power plant, Renew. Sustain. Energy Rev. 53 (2016) 1468–1485, https://doi.org/10.1016/j.rser.2015.09.051.

[14] Y. Shen, Rice husk silica derived nanomaterials for sustainable applications, Renew. Sustain. Energy Rev. 80 (February) (2017) 453–466, https://doi.org/10.1016/j.rser.2017.05.115.

[15] J.H. Lee, J.H. Kwon, J. Lee, H. Lee, J.H. Chang, B. Sang, Preparation of high purity silica originated from rice husks by chemically removing metallic impurities, J. Ind. Eng. Chem. (2017), https://doi.org/10.1016/j.jiec.2017.01.033.

[16] A. Siddika, A. Al Mamun, R. Alyousef, H. Mohammadhosseini, State-of-the-art-review on rice husk ash : a supplementary cementitious material in concrete, J. King Saud Univ. - Eng. Sci. (2020) 1–21, https://doi.org/10.1016/j.jksues.2020.10.006.

[17] K.S. Butler, J.I. Zink, C.J. Brinker, Synthetic amorphous silica nanoparticles: toxicity, biomedical and environmental implications, Nat. Rev. Mater. (2020) 1–24, https://doi.org/10.1038/s41578-020-0230-0.

[18] A.H. Thu, A.I. Zakharov, Preparation of inorganic binder for cold-hardening mixtures, Refract. Ind. Ceram. 59 (3) (2018) 313–317, https://doi.org/10.1007/s11148-018-0227-z.

[19] S. Gu, J. Zhou, Z. Luo, Q. Wang, M. Ni, A detailed study of the effects of pyrolysis temperature and feedstock particle size on the preparation of nanosilica from rice husk, Ind. Crop. Prod. 50 (2013) 540–549, https://doi.org/10.1016/j.indcrop.2013.08.004.

[20] R. Patil, R. Dongre, J. Meshram, Preparation of silica powder from rice, IOSR J. Appl. Chem. (2014) 26–29, no. January, www.iosrjournals.org.

[21] J.C. Furgal, C.U. Lenora, Green routes to silicon-based materials and their environmental implications, Phys. Sci. Rev. 2019 (24) (2019) 1–22, https://doi.org/10.1515/psr-2019-0024.

[22] H. Moayedi, B. Aghel, M.M. Abdullahi, H. Nguyen, A.S. A Rashid, Applications of rice husk ash as green and sustainable biomass, J. Clean. Prod. 237 (2019) 117851, https://doi.org/10.1016/j.jclepro.2019.117851.

[23] J. Zou, et al., Complementary use of generalized logistic mixture model and distributed activation energy model in exploring kinetic mechanisms of wheat straw and torrefied rice husk pyrolysis, J. Clean. Prod. 397 (February) (2023) 136560, https://doi.org/10.1016/j.jclepro.2023.136560.

[24] I. Glushankova, A. Ketov, M. Krasnovskikh, L. Rudakova, I. Vaisman, Rice hulls as a renewable complex material resource, Resources 7 (31) (2018) 1–11, https://doi.org/10.3390/resources7020031.

[25] R. Rathanasamy, et al., Influence of silicon dioxide-titanium dioxide antireflective electrosprayed coatings on multicrystalline silicon cells, Hindawi Adv. Mater. Sci. Eng. 2022 (2022).

[26] F. Unglaube, A. Lammers, C.R. Kreyenschulte, M. Lalk, E. Mejía, Preparation , characterization and antimicrobial properties of nanosized silver-containing carbon/silica composites from rice husk waste, Chem. Open 10 (2021) 1–7, https://doi.org/10.1002/open.202100239.

[27] M.Y. Nassar, I.S. Ahmed, M.A. Abo-raya, A facile and tunable approach for synthesis of pure silica nanostructures from rice husk for the removal of ciprofloxacin drug from polluted aqueous solutions, J. Mol. Liq. (2019), https://doi.org/10.1016/j.molliq.2019.03.017. #pagerange#.

[28] M.A. Al-Tameemi, M.V. Cherepanova, S.A. Smirnov, P.V. Skovorodnikov, Preparation of Silica from a Renewable Resource Rice, 2022.

[29] A.G. Adeniyi, T.E. Odetoye, J. Titiloye, J.O. Ighalo, A thermodynamic study of rice husk (Oryza Sativa) pyrolysis, Eur. J. Sustain. Dev. Res. 3 (4) (2019) 1–10, https://doi.org/10.29333/ejosdr/5830.

[30] K. Kaviyarasu, E. Manikandan, J. Kennedy, M. Jayachandran, M. Maaza, Rice husks as a sustainable source of high quality nanostructured silica for high performance Li-ion battery requital by sol-gel method – a review, Adv. Mater. Lett. 7 (9) (2016) 684–696, https://doi.org/10.5185/amlett.2016.6192.

[31] R. Abu Bakar, R. Yahya, S.N. Gan, Production of high purity amorphous silica from rice husk, Procedia Chem. 19 (2016) 189–195, https://doi.org/10.1016/j.proche.2016.03.092.

[32] G.M.K. Tolba, et al., Effective an highly recyclable nanosilica produced from the rice husk for effective removal of organic dyes, J. Ind. Eng. Chem. 29 (2015) 134–145, https://doi.org/10.1016/j.jiec.2015.03.025.

[33] X. Yao, K. Xu, Y. Liang, Comparing the thermo-physical properties of rice husk and rice straw as feedstock for thermochemical conversion and characterization of their waste ashes from combustion, Bioresources 11 (4) (2016) 10549–10564.

[34] S. Gu, J. Zhou, Z. Luo, Q. Wang, Z. Shi, Kinetic study on the preparation of silica from rice husk under various pretreatments, J. Therm. Anal. Calorim. 119 (2015) 2159–2169, https://doi.org/10.1007/s10973-014-4219-z.

[35] A.W. Putranto, S.H. Abida, A.B. Sholel, H.T. Azfa, The potential of rice husk ash for silica synthesis as a semiconductor material for monocrystalline solar cell : a review, IOP Conf. Ser. Earth Environ. Sci. 733 (2021) 1–10, https://doi.org/10.1088/1755-1315/733/1/012029.

[36] G.M.F. Gomes, C. Philipssen, E.K. Bard, L.D. Zen, G. De Souza, Rice husk bubbling fluidized bed combustion for amorphous silica synthesis, J. Environ. Chem. Eng. (2016) 1–47, https://doi.org/10.1016/j.jece.2016.03.049.

[37] S.S. Nekrashevich, V.A. Gritsenko, Electronic structure of silicon dioxide (A review), Phys. Solid State 56 (2) (2014) 209–223, https://doi.org/10.1134/S106378341402022X.

[38] S. Chandrasekhar, P.N. Pramada, J. Majeed, Effect of calcination temperature and heating rate on the optical properties and reactivity of rice husk ash, J. Mater. Sci. 41 (23) (2006) 7926–7933, https://doi.org/10.1007/s10853-006-0859-0.

[39] S. Sprenger, Epoxy resin composites with surface-modified silicon dioxide nanoparticles : a review, J. Appl. Polym. Sci. 130 (2013) 1421–1428, https://doi.org/10.1002/app.39208.

[40] K.G. Santhosh, S.M. Subhani, A. Bahurudeen, Recycling of palm oil fuel ash and rice husk ash in the cleaner production of concrete, J. Clean. Prod. 354 (March) (2022) 131736, https://doi.org/10.1016/j.jclepro.2022.131736.

[41] W. Gao, H. Li, Karnowo, B. Song, S. Zhang, Integrated leaching and thermochemical technologies for producing high-value products from rice husk : leaching of rice husk with the aqueous phases of bioliquids, Energies 13 (6033) (2020) 1–15, https://doi.org/10.3390/en13226033.

[42] C. Tsai, Y. Shen, W.-T. Tsai, Effect of alkaline pretreatment on the fuel properties of torrefied biomass from rice husk, Energies 16 (679) (2023) 1–10, https://doi.org/10.3390/en16020679.

[43] D. Chen, A. Gao, Z. Ma, D. Fei, Y. Chang, C. Shen, In-depth study of rice husk torrefaction : characterization of solid , liquid and gaseous products , oxygen migration and energy yield, Bioresour. Technol. 253 (December 2017) (2018) 148–153, https://doi.org/10.1016/j.biortech.2018.01.009.

[44] Z. Zhao, et al., Investigation on the fuel quality and hydrophobicity of upgraded rice husk derived from various inert and oxidative torrefaction conditions, Renew. Energy 189 (2022) (2022) 1234–1248, https://doi.org/10.1016/j.renene.2022.03.087.

[45] A.A. Franca, J. Schultz, R. Borges, F. Wypych, A.S. Mangrich, Rice husk ash as raw material for the synthesis of silicon and potassium slow-release fertilizer, J. Braz. Chem. Soc. 28 (11) (2017) 2211–2217, https://doi.org/10.21577/0103-5053.20170072.

[46] S. Echaroj, N. Pannucharoenwong, K. Duanguppama, M. Santikunaporn, P. Rattanadecho, Supercritical ethanol liquefaction of rice husk to bio-fuel over modified graphene oxide, Energy Rep. 8 (May) (2022) 173–183, https://doi.org/10.1016/j.egyr.2022.06.105.

[47] M. Patel, X. Zhang, A. Kumar, Techno-economic and life cycle assessment on lignocellulosic biomass thermochemical conversion technologies : a review, Renew. Sustain. Energy Rev. 53 (2016) 1486–1499, https://doi.org/10.1016/j.rser.2015.09.070.

[48] A. Bahramia, N. Soltania, M.I. Pech-Canula, C.A. Gutiérreza, Development of metal-matrix composites from industrial/agricultural waste materials and their derivatives, Crit. Rev. Environ. Sci. Technol. (2015) 1–130, https://doi.org/10.1080/10643389.2015.1077067. August 2015.

[49] A. Kasinathan, R. Rama, G. Sivakumar, Extraction , synthesis and characterization of nanosilica from rice husk ash, Int. J. Nanotechnol. Appl. 4 (1) (2010) 61–66.

[50] A. Bathla, C. Narula, R.P. Chauhan, Hydrothermal synthesis and characterization of silica nanowires using rice husk ash : an agricultural waste, J. Mater. Sci. Mater. Electron. 0 (0) (2018) 1–7, https://doi.org/10.1007/s10854-018-8598-y.

[51] O. Olawale, A.I. Akinmoladun, F.A. Oyawale, R. Atiko, Characterization of mono-crystalline silicon from rice husk ash, Int. J. Sci. Eng. Res. 4 (2) (2013) 1.

[52] A. Muthadhi, S. Kothandaraman, Optimum production conditions for reactive rice husk ash, Mater. Struct. 43 (2010) 1303–1315, https://doi.org/10.1617/s11527-010-9581-0.

[53] C.P. Draszewski, et al., Use of rice husk hydrolyzed by subcritical water to obtain silica from agro-industrial waste, Environ. Eng. Sci. 39 (12) (2022) 23–24, https://doi.org/10.1089/ees.2021.0501.

[54] A. Akter, et al., Immobilization of heavy metals in tannery sludge by the formation of tobermorite in subcritical water treatment with rice husk silica, RSC Adv. (2023) 10610–10620, https://doi.org/10.1039/d3ra00595j.

[55] M. Tangstad, Ferrosilicon and Silicon Technology, twelfth ed., Elsevier, 2013 https://doi.org/10.1016/B978-0-08-097753-9.00006-X.

[56] V.H. Le, C. Nhan, H. Thuc, H.H. Thuc, Synthesis of silica nanoparticles from Vietnamese rice husk by sol – gel method, Nanoscale Res. Lett. 8 (58) (2013) 1–10.

[57] F. Adam, J.N. Appaturi, A. Iqbal, The utilization of rice husk silica as a catalyst : review and recent progress, Catal. Today 190 (1) (2012) 2–14, https://doi.org/10.1016/j.cattod.2012.04.056.

[58] R. V Krishnarao, J. Subrahmanyam, T.J. Kumar, Studies on the formation of black particles in rice husk silica ash, J. Eur. Ceram. Soc. 21 (2001) 99–104.

[59] S. Chandrasekhar, K.G. Satyanarayana, P.N. Pramada, P. Raghavan, T.N. Gupta, Processing , properties and applications of reactive silica from rice husk — an overview, J. Mater. Sci. 8 (2003) 3159–3168.

[60] D. An, Y. Guo, Y. Zhu, Z. Wang, A green route to preparation of silica powders with rice husk ash and waste gas, Chem. Eng. J. 162 (2) (2010) 509–514, https://doi.org/10.1016/j.cej.2010.05.052.

[61] F. Wu, et al., One-step synthesis of Superbright water-soluble silicon nanoparticles with photoluminescence quantum yield exceeding 80 %,, Adv. Mater. Interfac. 2 (2015) 1–11, https://doi.org/10.1002/admi.201500360.

[62] P.P. Nayak, A.k. Datta, Synthesis of SiO 2 -nanoparticles from rice husk ash and its comparison with commercial amorphous silica through material characterization, Silicon (2020) 1–6, https://doi.org/10.1007/s12633-020-00509-y.

[63] M. Abou Rida, F. Harb, Synthesis and characterization of amorphous silica nanoparitcles from aqueous silicates uisng cationic surfactants, J. Met. , Mater. Miner. 24 (1) (2014) 37–42, https://doi.org/10.14456/jmmm.2014.7.

[64] H.B. Dizaji, T. Zeng, H. Holzig, J. Bauer, G. Kloß, D. Enke, Ash transformation mechanism during combustion of rice husk and rice straw, Fuel 307 (July 2021) (2022) 1–18, https://doi.org/10.1016/j.fuel.2021.121768.

[65] Y. Liu, H. Tan, Z. Tan, X. Cheng, Rice husk-derived carbon materials for aqueous Zn-ion hybrid supercapacitors, Appl. Surf. Sci. 608 (July 2022) (2023) 155215, https://doi.org/10.1016/j.apsusc.2022.155215.

[66] S.N.M. Raman, N.A. Ismail, S.S. Jamari, Preparation and characterization of impregnated commercial rice husks activated carbon with piperazine for carbon dioxide (CO 2) capture, IOP Conf. Ser. Mater. Sci. Eng. 206 (2017) 1–12, https://doi.org/10.1088/1757-899X/206/1/012005.

[67] P.L. Homagai, R. Poudel, S. Poudel, A. Bhattarai, Adsorption and removal of crystal violet dye from aqueous solution by modi fi ed rice husk, Heliyon 8 (January) (2022) e09261, https://doi.org/10.1016/j.heliyon.2022.e09261.

[68] A. Bahrami, M.I. Pech-Canul, C.A. Gutiérrez, N. Soltani, Applied Surface Science Wetting and reaction characteristics of crystalline and amorphous SiO 2 derived rice-husk ash and SiO 2/SiC substrates with Al – Si – Mg alloys, Appl. Surf. Sci. 357 (2015) 1104–1113, https://doi.org/10.1016/j.apsusc.2015.09.137.

[69] L. Kuo, W. Tsai, R. Yang, J.-H. Tsai, Production of high-porosity biochar from rice husk by the microwave pyrolysis process, Processes 11 (3119) (2023) 1–12, https://doi.org/10.3390/pr11113119.

[70] W. Gao, P. Xiao, G. Henkelman, K.M. Liechti, R. Huang, Interfacial adhesion between graphene and silicon dioxide by density functional theory with van der Waals corrections, J. Phys. D Appl. Phys. 47 (255301) (2014), https://doi.org/10.1088/0022-3727/47/25/255301, 6pp.

[71] J. Madhu, A. Santhanam, M. Natarajan, D. Velauthapillai, CO adsorption performance of template free zeolite A and X synthesized from rice husk ash as silicon source, RSC Adv. 12 (2022) 1–45, https://doi.org/10.1039/D2RA04052B.

[72] Y. Xu, B. Chen, Organic carbon and inorganic silicon speciation in rice-bran-derived biochars affect its capacity to adsorb cadmium in solution, J. Soils Sediments (2014) 1–11, https://doi.org/10.1007/s11368-014-0969-2.

[73] B. Satbaev, et al., Rice husk research : from environmental pollutant to a promising source of organo-mineral raw materials, Materials 14 (4119) (2021) 1–19, https://doi.org/10.3390/ma14154119.

[74] C.G. Flores, H. Schneider, J.S. Dornelles, L.B. Gomes, N.R. Marcilio, P.J. Melo, Synthesis of potassium zeolite from rice husk ash as a silicon source, Clean. Eng. Technol. 4 (June) (2021) 100201, https://doi.org/10.1016/j.clet.2021.100201.

[75] N. Thuadaij, A. Nuntiya, Preparation of nanosilica powder from rice husk ash by precipitation method, Chiang Mai J. Sci. 35 (1) (2008) 206–211.

[76] X. He, N. Zheng, R. Hu, Z. Hu, J.C. Yu, Hydrothermal and pyrolytic conversion of biomasses into catalysts for advanced oxidation treatments, Adv. Funct. Mater. 31 (7) (2021) 1–31, https://doi.org/10.1002/adfm.202006505.

[77] A. Zharmenov, et al., Production of refractory materials using a renewable source of silicon dioxide, Minerals 12 (1010) (2022) 1–23, https://doi.org/10.3390/min12081010.

[78] C.W. Lan, et al., Engineering silicon crystals for photovoltaics, CrystEngComm 18 (2016) 1474–1485, https://doi.org/10.1039/C5CE02343B.

[79] T. Okutani, View of Utilization of silica in rice hulls as raw materials for silicon semiconductors.pdf, J. Met. Mater. Miner. 19 (2) (2009) 51–59.

[80] Y. Katoh, L. Snead, Silicon carbide and its composites for nuclear applications – historical overview, J. Nucl. Mater. (2019) 151849, https://doi.org/10.1016/j.jnucmat.2019.151849.

[81] E. Bakan, Y.J. Sohn, R. Vaßen, Microstructure and phase composition evolution of silicon-hafnia feedstock during plasma spraying and following cyclic oxidation, Acta Mater. 214 (2021) 117007, https://doi.org/10.1016/j.actamat.2021.117007.

[82] V. De Waele, S. Mintova, Photoactive metal-containing zeolitic materials for sensing and light-to-chemical energy conversion, in: Chemistry of Silica and Zeolite-Based Materials, Elsevier Inc., 2019, pp. 331–350, https://doi.org/10.1016/B978-0-12-817813-3.00018-3.

[83] M.M. Rahman, N. Hasnida, W.B.W. Nik, Preparation of zeolite Y using local raw material rice husk as a silica source, J. Sci. Res. 1 (2) (2009) 285–291, https://doi.org/10.3329/jsr.v1i2.1777.

[84] M. Deng, G. Zhang, X. Peng, J. Lin, X. Pei, R. Huang, A facile procedure for the synthesis of δ -Na2Si2O5 using rice husk ash as silicon source, Mater. Lett. 163 (2016) 36–38, https://doi.org/10.1016/j.matlet.2015.10.046.

[85] S. Muthukrishnan, S. Gupta, H.W. Kua, Application of rice husk biochar and thermally treated low silica rice husk ash to improve physical properties of cement mortar, Theor. Appl. Fract. Mech. (2019) 102376, https://doi.org/10.1016/j.tafmec.2019.102376.

[86] Q. Feng, H. Yamamichi, M. Shoya, S. Sugita, Study on the pozzolanic properties of rice husk ash by hydrochloric acid pretreatment, Cement Concr. Res. 34 (2004) 521–526, https://doi.org/10.1016/j.cemconres.2003.09.005.

[87] Y. Jin, et al., Amorphous silica nanohybrids : synthesis , properties and applications, Coodination Chem. Rev. 253 (2009) 2998–3014, https://doi.org/10.1016/j.ccr.2009.06.005.

[88] R. Narayan, U.Y. Nayak, Mesoporous silica nanoparticles : a comprehensive review on synthesis and recent advances, Pharmaceutics 10 (118) (2018) 1–49, https://doi.org/10.3390/pharmaceutics10030118.

[89] M. Ali, A.A. Drea, Green synthesis and characterization of antibiotic amorphous nano silicon oxide powder extracted from rice husk ash, Int. J. Curr. Res. Rev. (January) (2022) 1–7, https://doi.org/10.31782/IJCRR.2021.132406.